Space-time picture of ultrarelativistic nuclear collisions

Yuri Sinyukov

Part 3

The thermodynamic arias occupied by different forms of the matter

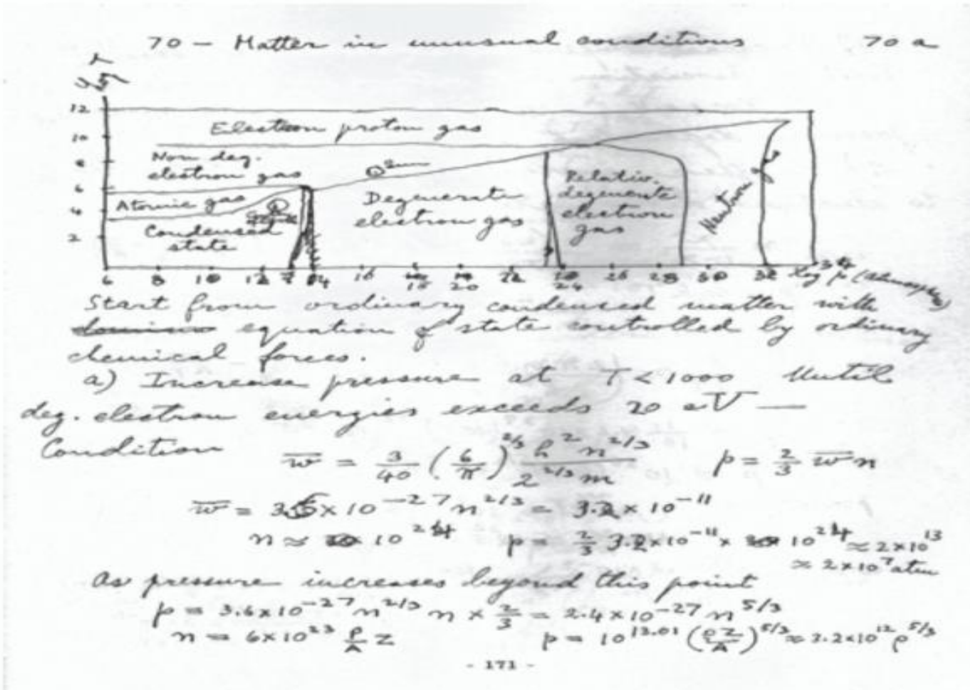

1953 Enrico Fermi

1983 US long range plan, Gordon Baym

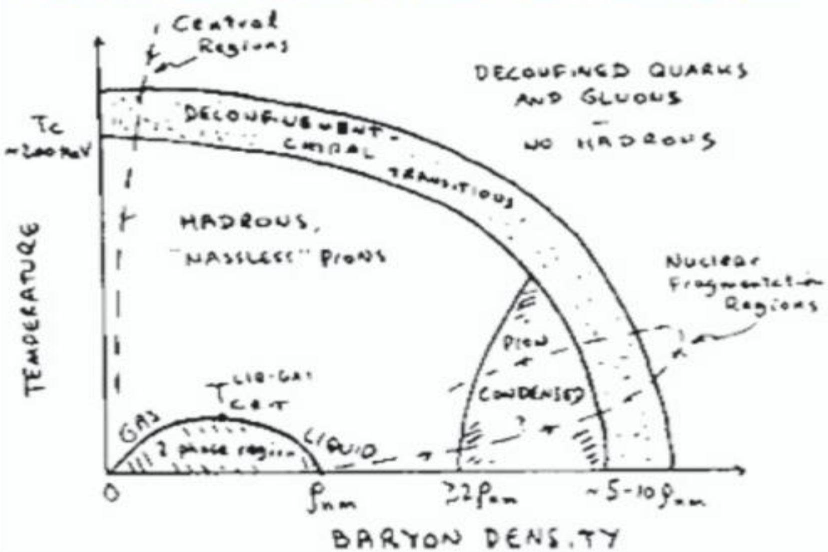

Larry McLerran '09

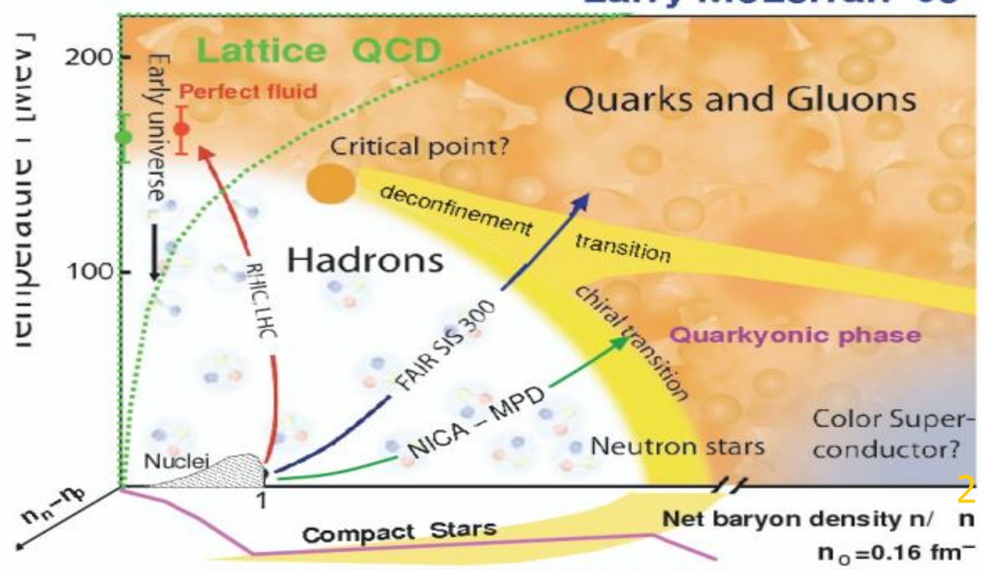

Heavy Ion Experiments

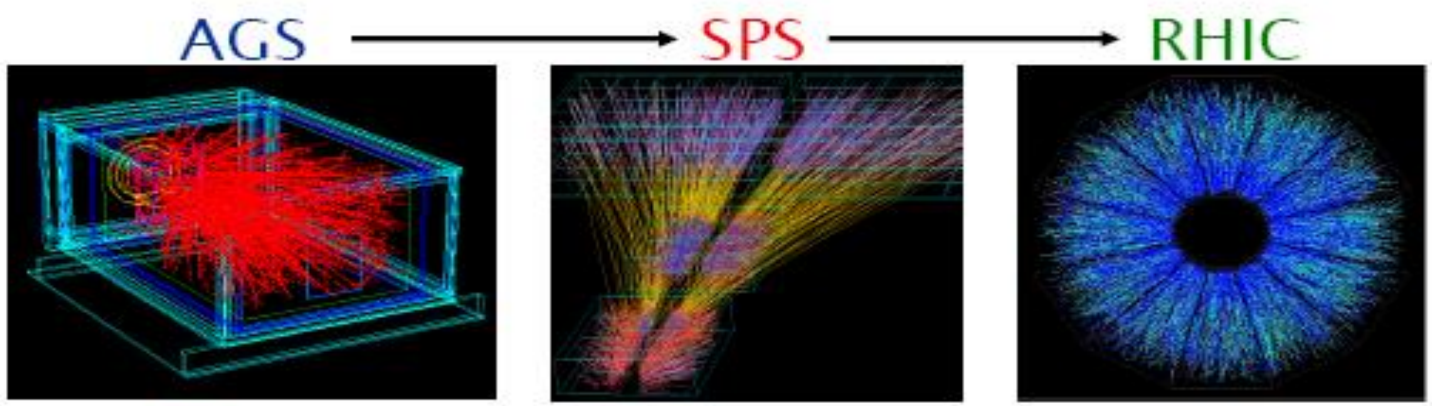

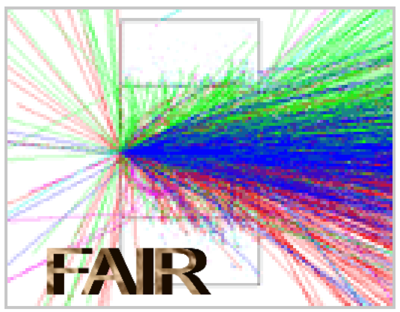

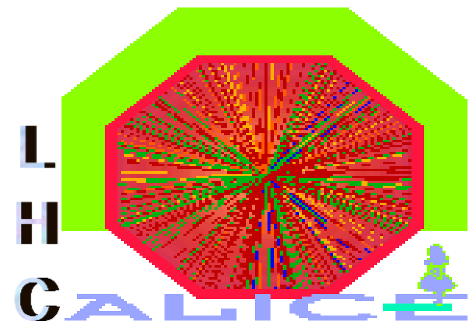

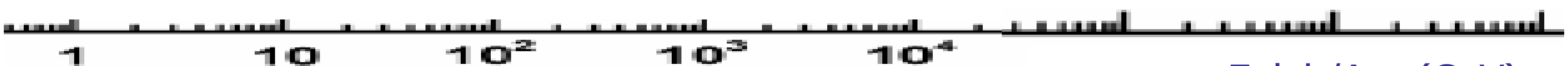

E_lab/A (GeV)

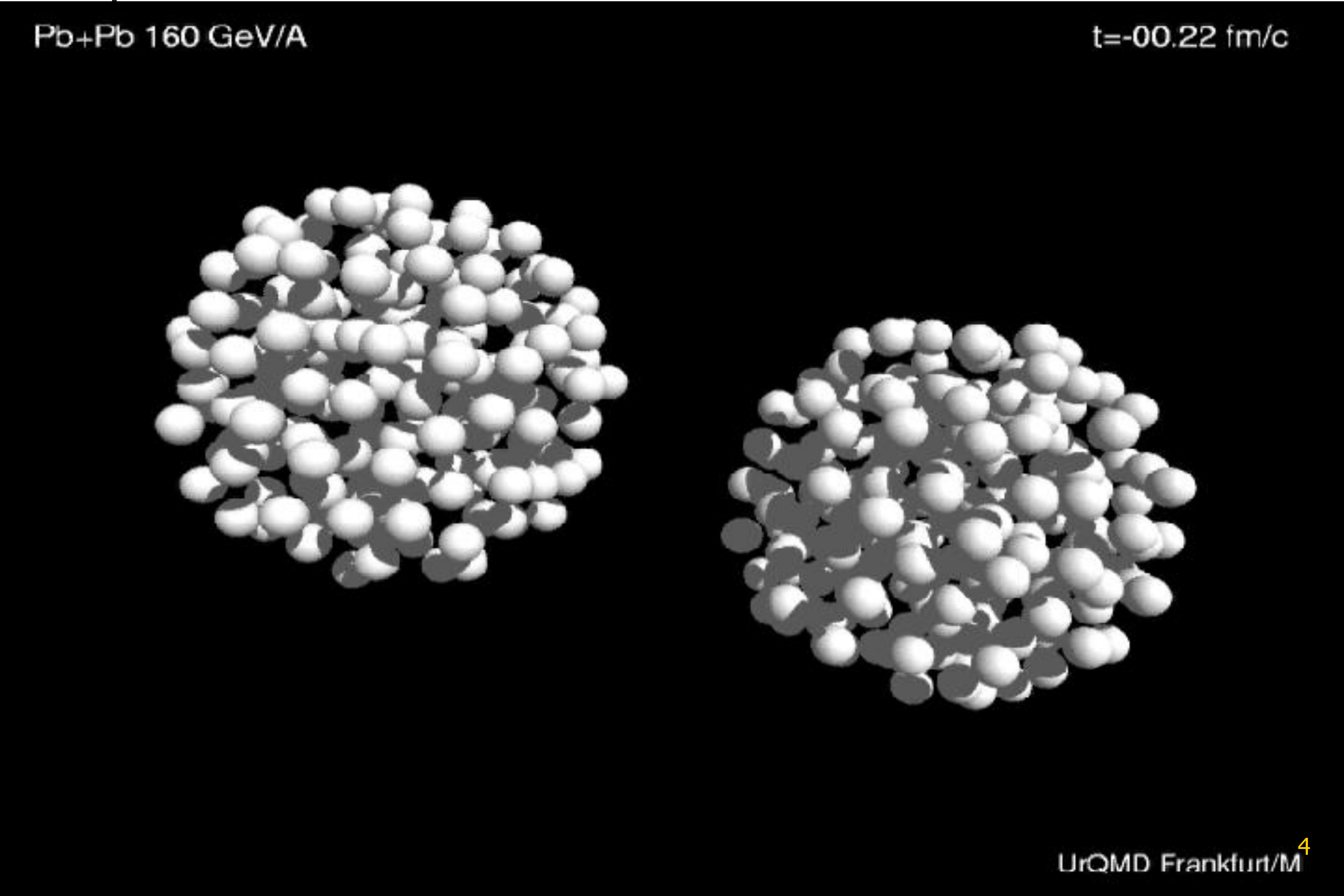
Pb+Pb 160 GeV/A
t=-00.22 fm/c
UrQMD Frankfurt/M

The cartoon of relativistic heavy ion collisions

At the start ====>

At the end====>

Temporal dependence of the pressure and temperature ======>

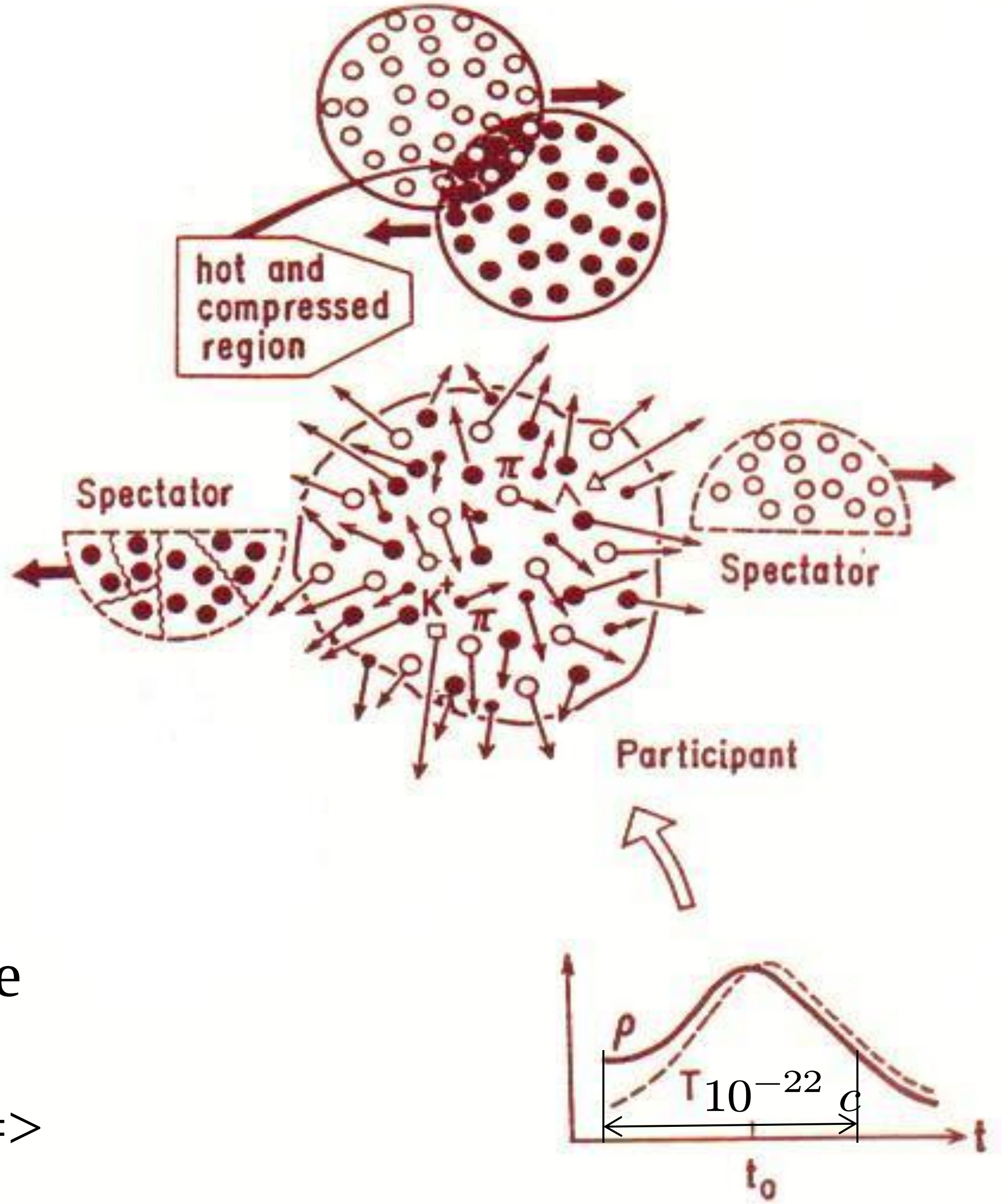

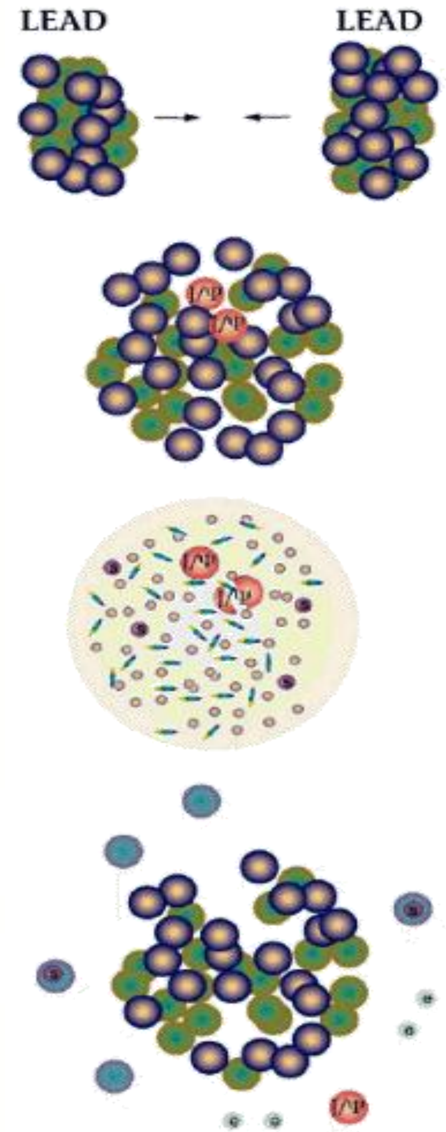

“Soft Physics” measurements

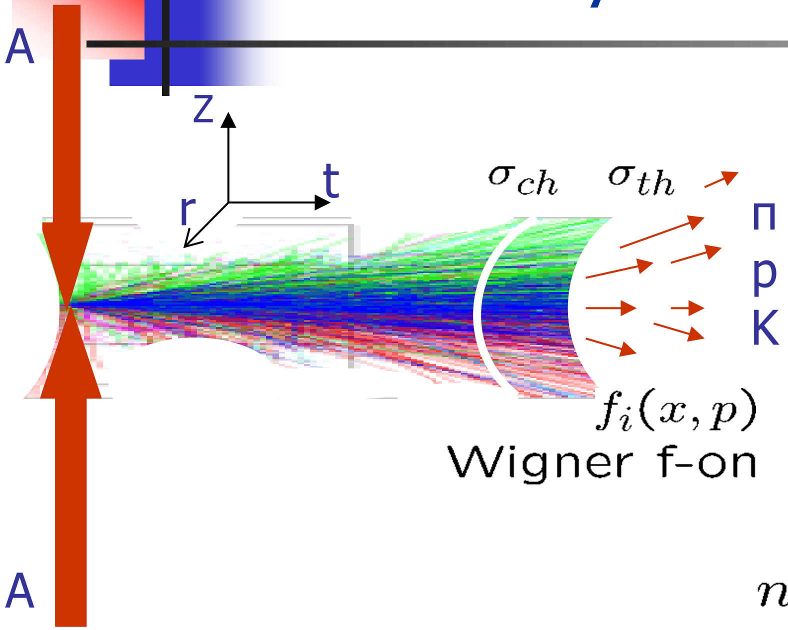

$T_{f.o.}$

Landau, 1953

$\sigma_{f.o.}$

$$N_i = \int \frac{d^3p}{p^0} d\sigma_\mu p^\mu f_i(x,p) \quad d^3xp^0$$

$$n_i(p) \equiv p^0 \frac{d^3N_i}{d^3p} = \int d\sigma_\mu p^\mu f_i(x,p)$$

$$\sim e^{-\sqrt{m_i^2+p_T^2}/T_{eff,i}}$$

$$n_i(p_1,p_2) \equiv p_1^0 p_2^0 \frac{d^6N_i}{d^3p_1 d^3p_2} = C(p,q) n(p_1) n(p_2)$$

$p=(p_1+p_2)/2$

$q=p_1-p_2$

$\{\frac{N_i}{N_j}\}$ → T_{ch} and μ_{ch} soon after hadronization (chemical f.o.)

$$\frac{d^3N}{dp_t\,dy\,d\varphi} = \frac{d^2N}{dp_t\,dy}\frac{1}{2\pi}(1+2v_1\cos(\varphi)+2v_2\cos(2\varphi)+\ldots)$$

Directed flow

Elliptic flow

Radial flow → $T_{eff,i} \approx T_{f.o.} + m_i \frac{\langle v_T{}^2\rangle}{2}$

Inverse of spectra slope

QS Correlation function

$$1+\lambda\exp(-R_L(p)^2q_L^2 - R_S^2(p)^2q_S^2 - R_O^2(p)q_O^2)$$

Space-time structure of the matter evolution, e.g.,

$$\tau \approx R_L\sqrt{\frac{m_T}{T_{f.o.}}}$$

Interferometry microscope (*Kopylov / Podgoretcky - 1971*)

The idea of the correlation femtoscopy is based on an impossibility to distinguish between registered identical particles emitted from different points.

t=0

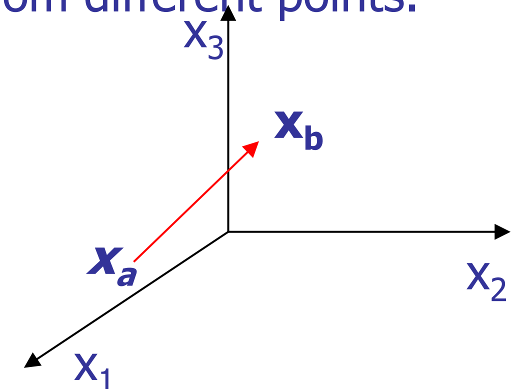

$$f(x) = \exp[-\sum \frac{x_i^2}{2R_i^2}]$$

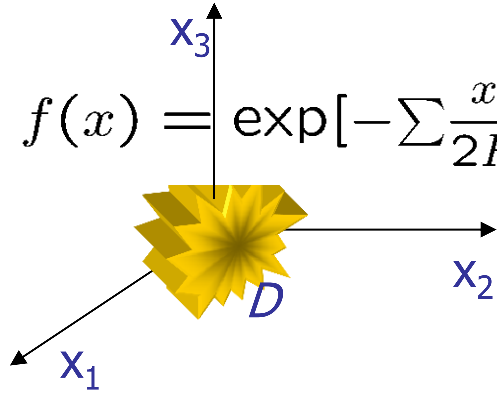

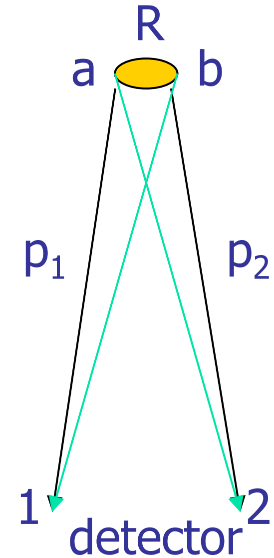

Momentum representation

$$\Psi_{x_a,x_b}(p_1,p_2) = \frac{1}{\sqrt{2}}\left[e^{-i\mathbf{p}_1\cdot\mathbf{x}_a}e^{-i\mathbf{p}_2\cdot\mathbf{x}_b} \pm e^{-i\mathbf{p}_2\cdot\mathbf{x}_a}e^{-i\mathbf{p}_1\cdot\mathbf{x}_b}\right]$$

Probabilities:

$$W_{x_a,x_b}(p_1,p_2) = |\Psi_{x_a,x_b}(p_1,p_2)|^2 = 1 \pm \cos[\underbrace{(\mathbf{p}_1 - \mathbf{p}_2)}_{\mathbf{q}} \cdot (\mathbf{x}_a - \mathbf{x}_b)]$$

$$W_D(p_1,p_2) = \int d^3x_a d^3x_b f(x_a) f(x_b) W_{x_a,x_b}(p_1,p_2) =$$

$$1 \pm |\int d^3x f(x) e^{i\mathbf{qx}}|^2 = 1 \pm \exp\left[-\sum q_i^2 R_i^2\right]$$

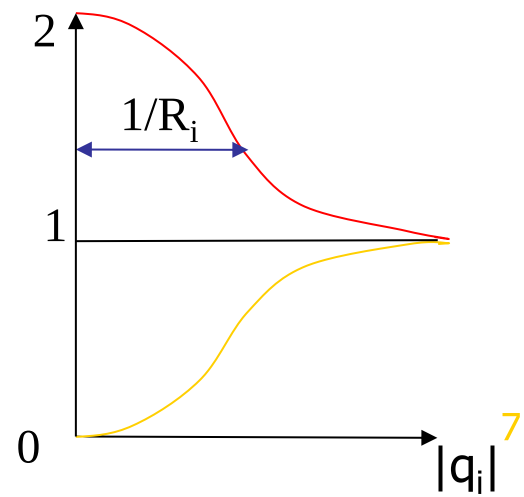

THE DEVELOPMENT OF THE FEMTOSCOPY

- Even ultra small systems can have an internal structure.
  Then the distribution function *f(x,p)* and emission function of such an objects are inhomogeneous and, typically, correlations between the momentum *p* of emitted particle and its position x appear.
- **In this case and in general the interferometry microscope measure the homogeneity lengths in the systems** [Yu. Sinyukov , 1986, 1993-1995].

$$\frac{|f(p,x_0+\bar{\lambda})-f(p,x_0)|}{f(p,x_0)}=\frac{1}{2} \quad \text{at} \quad \left.\frac{\partial f(p,x)}{\partial x_i}\right|_{x_0(p)}=0 \quad \Longrightarrow \quad \lambda_i^2=\frac{f(x_0,p)}{|f''_{x_i}(x_0,p)|}$$

In hydrodynamic situation the distribution functions on *x* and *p* are not factorized. They are entangled, correlated:

$$f(x,p)=f(p)\exp(-\sum\frac{x_i^2}{2R_i^2}) \rightarrow \frac{1}{(2\pi)^3}[\exp(\frac{p^\mu u_\mu(x)}{T(x)}-\frac{\mu(x)}{T(x)})-1]^{-1}$$

Correlations functions are defined through thermal Wick`s theorem

$$p^0\frac{dN}{d\mathbf{p}}=\langle a_p^+a_p\rangle,\quad p_1^0p_2^0\frac{dN}{d\mathbf{p}_1d\mathbf{p}_2}=\langle a_{p_1}^+a_{p_2}^+a_{p_1}a_{p_2}\rangle$$

$$C(p_1,p_2)=1+\langle a_{p_1}^+a_{p_2}\rangle\langle a_{p_2}^+a_{p_1}\rangle/\langle a_{p_1}^+a_{p_1}\rangle\langle a_{p_2}^+a_{p_2}\rangle$$

$$\langle a_{p_1}^+a_{p_2}\rangle=\int_{\sigma_{out}}d\sigma_\mu(x)\,p^\mu\exp(iqx)\,f_{esc}(x,p)$$

THE DEVELOPMENT OF THE FEMTOSCOPY (Yu.S.1986 – 1995)

To provide calculations analytically one should use the saddle point method and Boltzmann approximation to Bose-Einstein distribution function. Then the single particle spectra are proportional to homogeneity volume:

$$p^0 \frac{d^3N}{d^3p} \propto \prod_i \lambda_i(p)$$

and just these homogeneity lengths forms exponent in Bose-Einstein correlation function

$$C = 1 + \exp\left[-\sum q_i^2 R_i(p)^2\right]$$

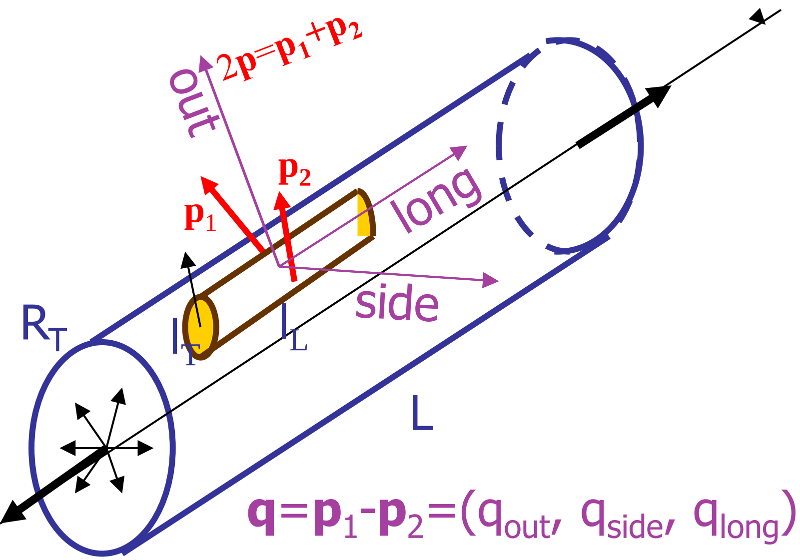

Interferomerty radii:

$$R_L(p_T) \approx \lambda_L = \tau\sqrt{\frac{T_{f.o.}}{m_T}}/cosh(y), m_T = \sqrt{m^2 + p_T^2}$$

$$R_S \approx \lambda_T = R_T/\sqrt{1 + Im_T/T_{f.o.}},\ I \propto < v_T^2 >$$

$$R_o^2 \approx \lambda_T^2 + v^2\langle\triangle t^2\rangle_p - 2v\langle\triangle x_o \triangle t\rangle_p, v = \frac{p_{out}}{p_0}$$

$$C(p,q) = \frac{d^6N/d^3p_1 d^3p_2}{d^3N/d^3p_1 d^3N/d^3p_2} \approx 1 + e^{R_L^2(p)q_L^2 + R_s^2(p)q_s^2 + R_O^2(p)q_O^2}$$

QGP → $R_{out}/R_{side} >> 1$ $Exp : R_{out}/R_{side} \approx 1$ RHIC HBT PUZZLE

Correlation femtoscopy of nucleus-nucleus collsions

- The femtoscopy analysis is used by Collaborations at SPS, RHIC and LHC. They provide the measurements of the space-time scales in the expanding matter with accuracy 10^{-15} m and 10^{-23} c.

Some basic points

«Sinyukov-Makhlin formula" for an estimate of the duration of "Little Bang"

$$\tau \approx R_L \sqrt{\frac{m_T}{T_{f.o.}}}$$ (1987)

$$R_l^2(k_T) = \tau^2 \lambda^2 \left(1 + \frac{3}{2}\lambda^2\right)$$

2015

$$\lambda^2 = \frac{T}{m_T}\left(1 - \bar{v}_T^2\right)^{1/2}$$

Femto "**homogeneity lengths**" general interpretation of the femtoscopy measurements as "homogeneity lenghts" (1993)

$$\lambda_i^{\,2} = \frac{f(x_0, p)}{\left|f''_{x_i}(x_0, p)\right|}$$

"Bowler–Sinyukov treatment" extracts the femtoscopic correlations from effects of the Coulomb interactions and long-lived resonances (1998)

$C(\mathbf{q})=[(1-\lambda)+\lambda K(q\_inv)(1+G(\mathbf{q}))]$

The evidences of space-time evolution of the thermal matter in A+A collisions:

- Rough estimate of the fireball lifetime for Au+Au $\sqrt{s} = 200$ Gev:

$$R_L(p_T, y=0) \approx \tau \sqrt{\frac{T_{f.o.}}{m_T}} \quad (m_T \gg T_{f.o.}) \quad \Longrightarrow \quad \tau > 10 \text{ fm/c}$$

$$\text{for } m_T = \sqrt{m^2 + p_T^2} = 1.75 \text{ GeV}$$

In p+p all femto-scales are of order 1 fm ! ⟹ A+A is not some kind of superposition of the individual collisions of nucleons of nuclei

The phenomenon of space-time *evolution* of the strongly interacting matter in A+A collisions

What is the nature of this matter at the early collision stage?
Whether does the matter becomes thermal?

Particle number ratios are well reproduced in thermal gas model with 2 parameters: *T*, μ_B for collision energies from AGS to RHIC:
thermal+chemical equilibrium

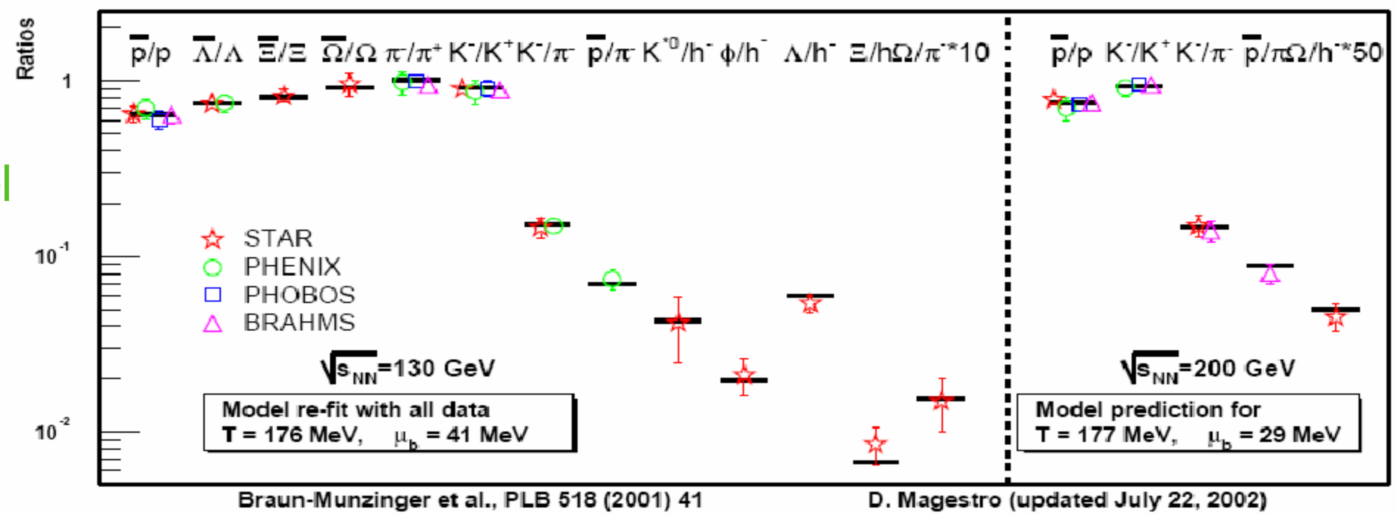

Collective expansion of the fireball.

- Observation of the longitudinal expansion:

$$R_L(p_T, y) \approx \tau \sqrt{\frac{T_{f.o.}}{m_T}} / \cosh(y)$$

It was conformed by NA35/NA49 Collaborations (CERN), 1995 !

- Observation of transverse (radial) collective flows:

Effective temperature for different particle species (inverse of the slope) p_T<m:

$$T_{eff} = T_{f.o.} + \frac{m<v^2>}{2}$$

radial collective flow

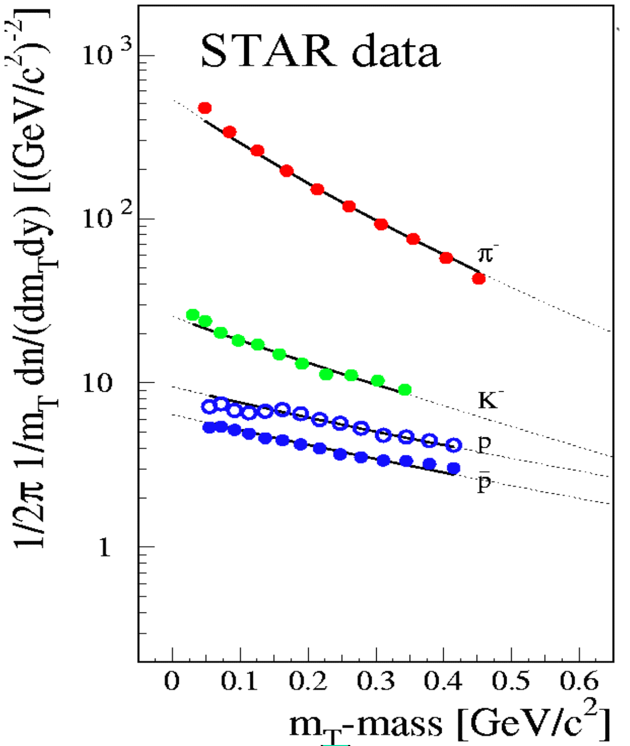

- Observation of elliptic flows:

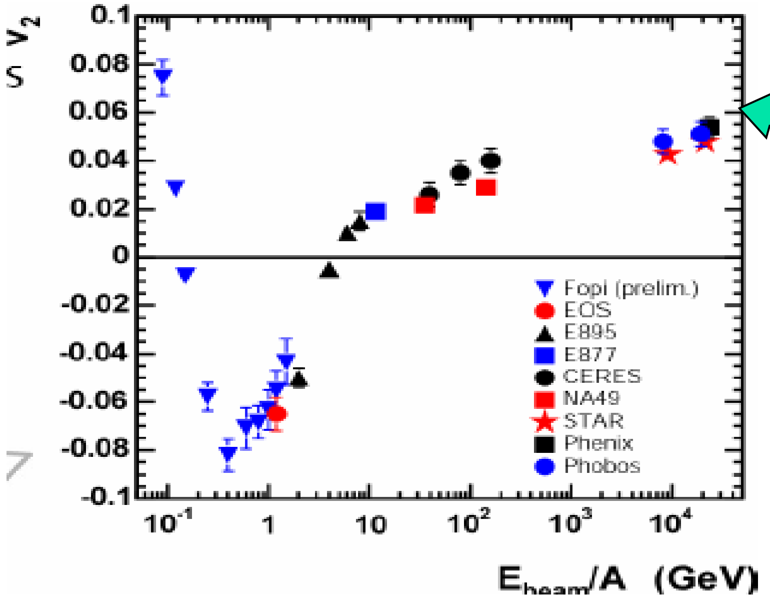

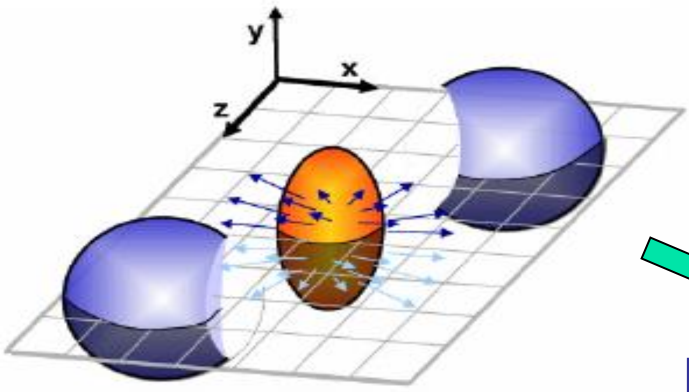

HYDRODYNAMICS !

Empirical observations and theoretical problems

- The creation of the superdence matter with $\epsilon > 100\ \epsilon_{nucl}$ is observed at RHIC and LHC
- The thermalization of such a matter is seen in the particle yields, spectra and correlations.
- Hydrodynamics describe well the soft physics (bulk matter observables).
- The letter means an existence of a new form of thermal matter at the temperatures T=155-350 MeV : asymptotically free QGP ⟹ strongly coupled sQGP, or quark-gluon fluid.

THEORETICAL PROBLEM

- An satisfying description of elliptic flows at RHIC requires the earlier thermalization, $\tau_{th} \simeq 0.4 fm/c$ and almost perfect fluid . At the same time the most optimistic estimates give thermalization time 1-1.5 fm/c.
- QGP and experimental ratio: $R_{out}/R_{side} \approx 1$ ⟹ **HBT Puzzle**

Space-time picture of ultrarelativistic nuclear collisions

Yuri Sinyukov

Part 4

Pre-thermal transverse flow

Initial flows and Ro/Rs ratio (t_0=1-2 fm/c)

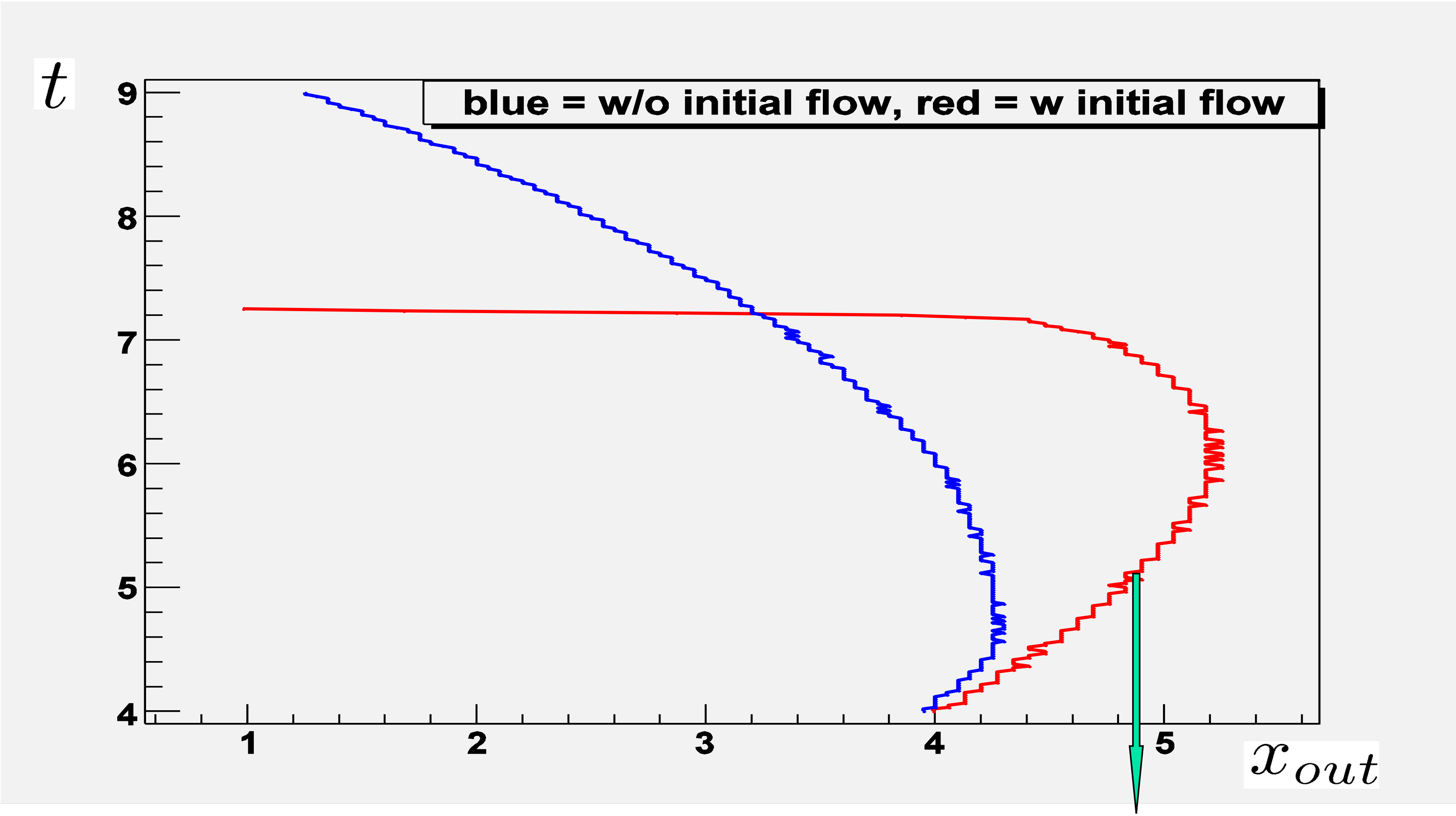

$$R_{out}^2 \approx R_{side}^2 + v^2\langle\triangle t^2\rangle_p - 2v\langle\triangle x_{out}\triangle t\rangle_p, v = \frac{p_T}{p^0}$$

Way to clarify the problems

Analysis
of evolution of observables in hydrodynamic and kinetic models of A+A collisions

Yu.M. Sinyukov, S.V.Akkelin, Y. Hama: Phys. Rev. Lett. 89, 052301 (2002);

S.V.Akkelin. Yu.M. Sinyukov: Phys. Rev. C **70** , 064901 (2004);
Phys.Rev. C **73**, 034908 (2006);
Nucl. Phys. A (2006) in press

N.S. Amelin, R. Lednicky, L. V. Malinina, T. A. Pocheptsov and Yu.M. Sinyukov:
Phys.Rev. C **73**, 044909 (2006)

Particle spectra and correlations

- Inclusive spectra

$$p^0 \frac{dN}{d\mathbf{p}} \equiv n(p) = \left\langle a_p^+ a_p \right\rangle, \quad p_1^0 p_2^0 \frac{dN}{d\mathbf{p}_1 d\mathbf{p}_2} \equiv n(p_1, p_2) = \left\langle a_{p_1}^+ a_{p_2}^+ a_{p_1} a_{p_2} \right\rangle$$

- Chaotic source

$$n(p_1, p_2) = \langle a_{p_1}^+ a_{p_1} \rangle \langle a_{p_2}^+ a_{p_2} \rangle + \langle a_{p_1}^+ a_{p_2} \rangle \langle a_{p_2}^+ a_{p_1} \rangle$$

- Correlation function

$$C(p_1, p_2) = n(p_1, p_2) / n(p_1) n(p_2)$$

- Irreducible operator averages:

$$\left\langle a_{p_1}^+ a_{p_2} \right\rangle = \int_{\sigma_{out}} d\sigma_\mu p^\mu \exp(iqx) f(x, p); \quad p = (p_1 + p_2)/2, \; q = p_1 - p_2$$

Escape probability

- **Boltzmann Equation:** $$\frac{p^\mu}{p^0}\frac{\partial f(x,p)}{\partial x^\mu} = F^{gain}(x,p) - F^{loss}(x,p)$$

rate of collisions

$$F^{loss}(x,p) = R(x,p)\, f(x,p) \quad \text{where} \quad R(x,p) = \langle \sigma v_{rel} \rangle n(x)$$

- **Escape probability (at $\bar{t}_\sigma \to \infty$):**

$$\mathcal{P}_{\bar{\sigma}}(x,p) = \exp\left(- \int_t^{t_\sigma} dt' R(x',p) \right) = \mathcal{P}_{t \to t_\sigma}$$

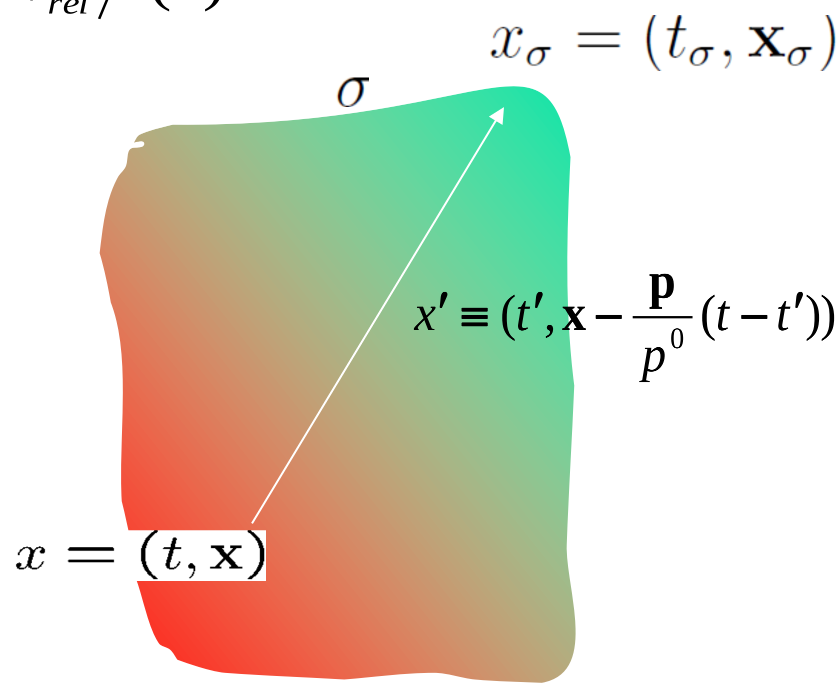

Distribution and emission functions

- Integral form of Boltzmann equation

$$f(t,\mathbf{x},p) = f\left(t_0,\mathbf{x}-\frac{\boldsymbol{p}}{p^0}(t-t_0),p\right)\mathcal{P}_{t_0\to t}\left(t_0,\mathbf{x}-\frac{\boldsymbol{p}}{p^0}(t-t_0),p\right)$$
$$\int_{t_0}^{t} F_{gain}\left(\tau,\mathbf{x}-\frac{\boldsymbol{p}}{p^0}(t-\tau),p\right)\mathcal{P}_{\tau\to t}\left(\tau,\mathbf{x}-\frac{\boldsymbol{p}}{p^0}(t-\tau),p\right)d\tau$$

- Operator averages

Distribution function

$$\langle a^{+}_{p_1} a_{p_2}\rangle|_\sigma = \int_\sigma d^3\sigma_\mu(x)p^\mu e^{iqx} f(x,p) =$$

$$\int_{\sigma_0} d^3\sigma_\mu(x_0)p^\mu f(x_0,p)\mathcal{P}_\sigma(x,p)e^{iqx_0} + \int_{\sigma_0}^{\sigma} d^4x e^{iqx} p^0 F_{gain}(x,p)\mathcal{P}_\sigma(x,p)$$

Emission function: $S_0^\mu(x_0,p)$ Initial emission; $S(x,p)$ Emission density

Dissipative effects & Spectra formation

$$\frac{p^{\mu}}{p^{0}}\frac{\partial f(x,p)}{\partial x^{\mu}} = F^{gain}(x,p) - F^{loss}(x,p)$$

$$\partial_{\mu}\left[p^{\mu}\exp(iqx)\right] = 0$$

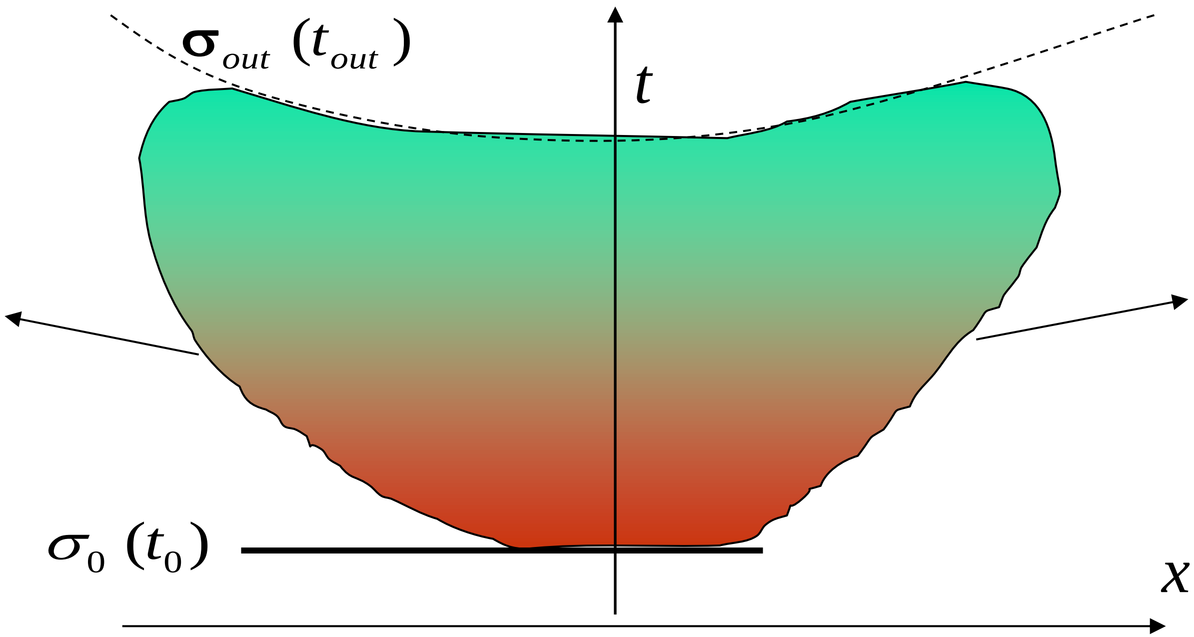

$$\left\langle a^{+}_{p_1} a_{p_2} \right\rangle = p^{\mu}\int_{\sigma_0} d\sigma_{\mu} f(x,p)\, e^{iqx} + p^{0}\int_{\sigma_0}^{\sigma_{out}} d^4x \left(F^{gain}(x,p) - F^{loss}(x,p)\right)e^{iqx}$$

Solution of Boltzmann equation for locally equilibrium expanding fireball

$$f(t,\mathbf{x},\mathbf{v}) = \frac{N}{(2\pi R_0)^3}\left(\frac{m}{T_0}\right)^{\frac{3}{2}} \exp\left(-\frac{m\mathbf{v}^2}{2T_0} - \frac{(\mathbf{x}-\mathbf{v}t)^2}{2R_0^{\ 2}}\right)$$

$\Vert$

$$f(t,\mathbf{x},\mathbf{v}) = \frac{N}{(2\pi R_0)^3}\left(\frac{m}{T_0}\right)^{\frac{3}{2}} \exp\left(-\frac{\mathbf{x}^2}{2R(t)^2} - \frac{m(\mathbf{v}-\mathbf{u}(t,\mathbf{x}))^2}{2T(t)}\right)$$

$$\mathbf{u} = \mathbf{x}\frac{tT_0}{mR_0^2 + T_0 t^2}$$

$$\frac{\partial f(t,\mathbf{x},\mathbf{v})}{\partial t} + \mathbf{v}\frac{\partial f(t,\mathbf{x},\mathbf{v})}{\partial \mathbf{x}} = 0$$

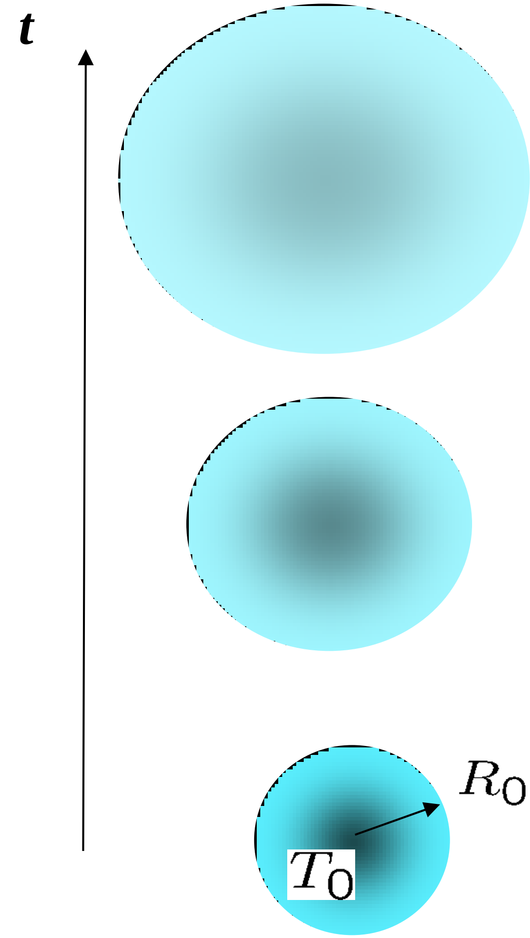

The spectra and interferometry radii do not change:

- One particle velocity (momentum) spectrum

$$f(t,\mathbf{v}) = N\left(\frac{m}{2\pi T_0}\right)^{\frac{3}{2}} \exp\left(-\frac{m\mathbf{v}^2}{2T_0}\right) = \underline{f(t=0,\mathbf{v})}$$

- Two particle correlation function

$$C(t,q) = 1 + \frac{\left|\langle a_{p_1}^{+} a_{p_2}\rangle\right|^2}{\langle a_{p_1}^{+} a_{p_1}\rangle\langle a_{p_2}^{+} a_{p_2}\rangle} = 1 + \exp(-q^2 R_0^2) = \underline{C(t=0,q)}$$

Collective velocities developed between τ_0=0.3 and τ=1.0 fm/c

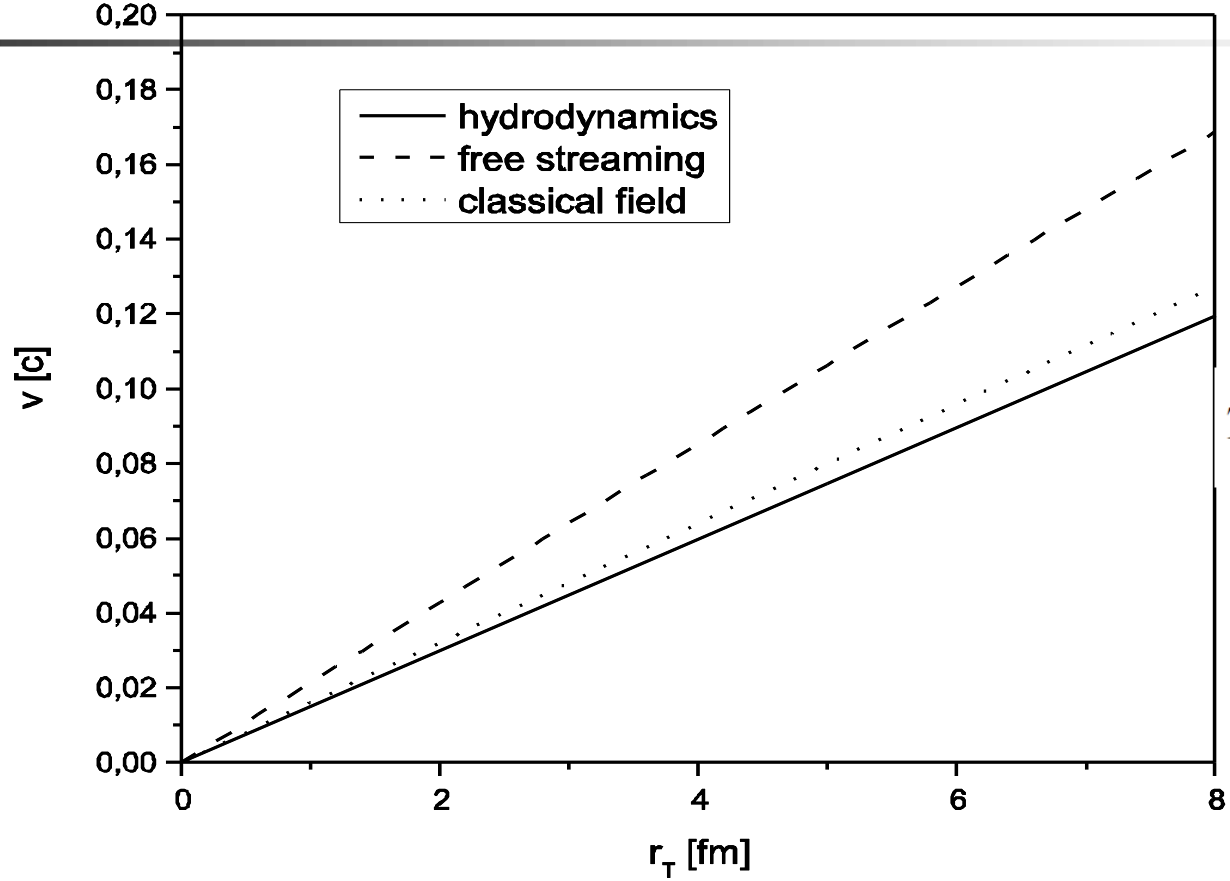

Central collisions

$$T^{\mu\nu}(x) = \int d^3p \frac{p^\mu p^\nu}{p_0} f(x,p)$$

$$u^\mu = \frac{T^{\mu\nu}u_\nu}{T^{\mu\nu}u_\mu u_\nu} = \frac{T^{\mu\nu}u_\nu}{\epsilon}$$

Collective velocity developed at pre-thermal stage from proper time tau_0 =0.3 fm/c by supposed thermalization time tau_th = 1 fm/c for scenarios of partonic free streaming and free expansion of classical field. The results are compared with the hydrodynamic evolution of perfect fluid with hard equation of state p = 1/3 epsilon started at τ_0 . Impact parameter b=0.

Yu.S. Acta Phys.Polon. B37 (2006) 3343; Gyulassy, Yu.S., Karpenko, Nazarenko Braz.J.Phys. 37 (2007) 1031. Yu.S., Nazarenko, Karpenko: Acta Phys.Polon. B40 1109 (2009) .

Collective velocities and their anisotropy developed between τ_0=0.3 and τ =1.0 fm/c

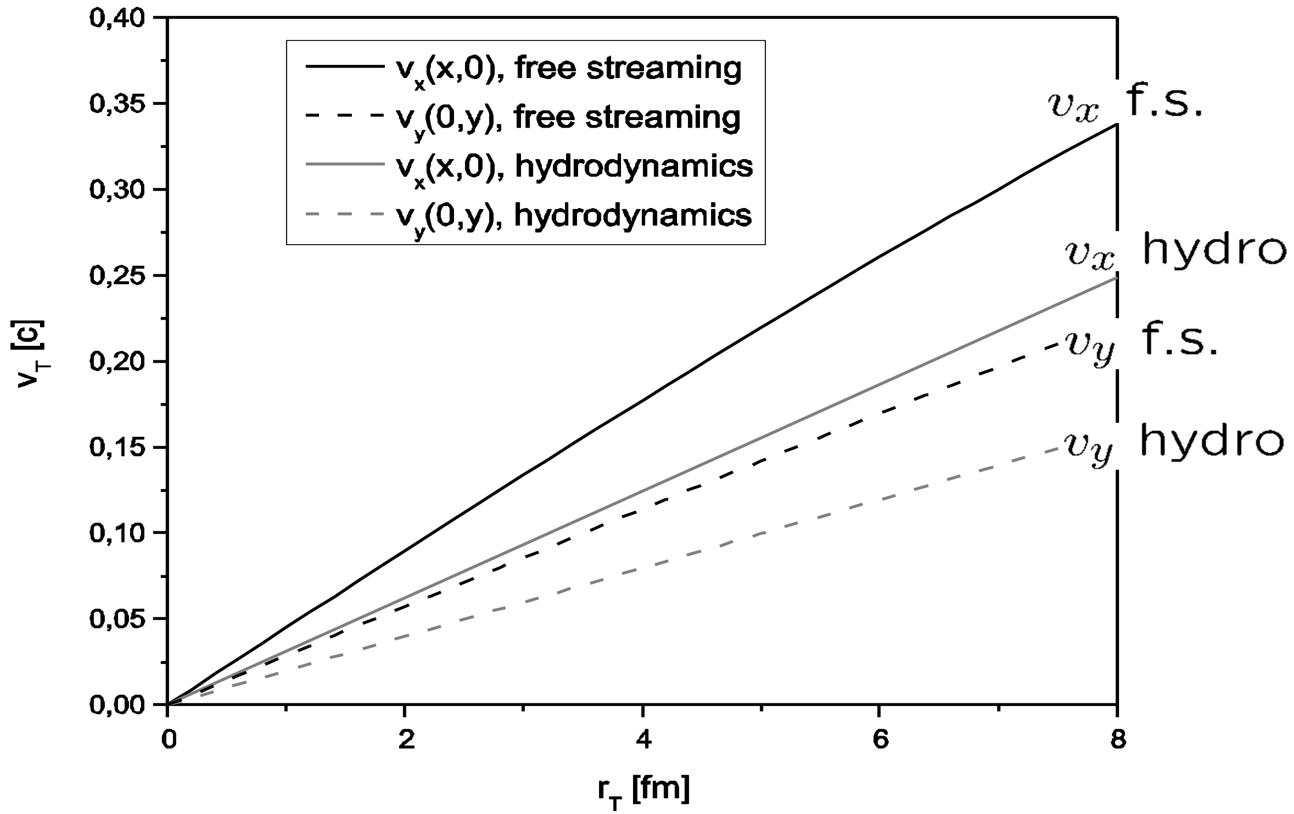

Non-central collisions
b=6.3 fm

Collective velocity developed at pre-thermal stage from proper time τ_0=0.3 fm/c by supposed thermalization time tau_i = 1 fm/c for scenarios of partonic free streaming. The results are compared with the hydrodynamic evolution of perfect fluid with hard equation of state p = 1/3 epsilon started at τ_0 . Impact parameter b=6.3 fm.

Yu.S. Acta Phys.Polon. B37 3343 (2006);
Yu.S., Nazarenko, Karpenko: Acta Phys.Polon. B40 1109 (2009)

- **The initial transverse flow in thermal matter as well as its anisotropy are developed at pre-thermal - either partonic, string or classical field (glasma) - stage with even more efficiency than in the case of very early perfect hydrodynamics.**

- **Such radial and elliptic flows develop no matter whether a pressure already established. The general reason for them is an essential finiteness of the system in transverse direction.**

- **The anisotropy of the flows transforms into asymmetry of the transverse momentum spectra only of (partial) thermalization happens.**

- **So, the results, first published in 2006, show that whereas the assumption of (partial) thermalization in relativistic A + A collisions is really crucial to explain soft physics observables, the hypotheses of early thermalization at times less than 1 fm/c is not necessary.**

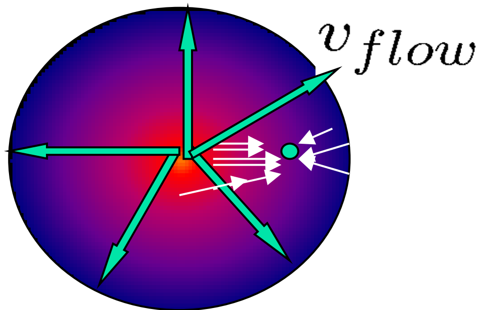

$$v_{flow,i} \sim r_i t/\lambda^2_{homog,i}$$

The relaxation model of the matter thermalization in A+A collisions

Expecting Stages of Evolution in Ultrarelativistic A+A collisions

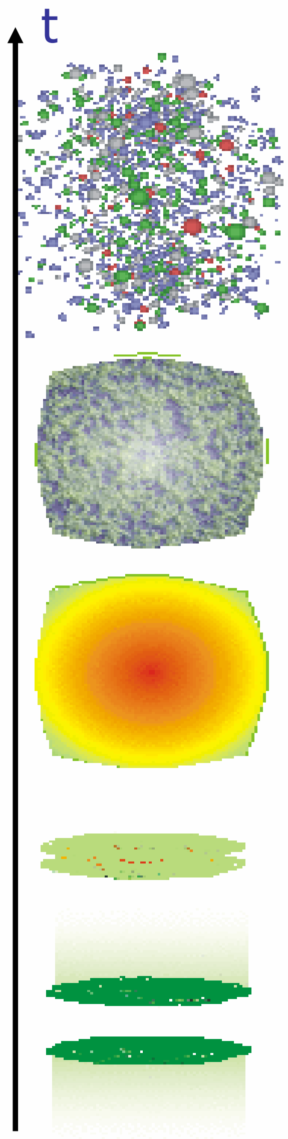

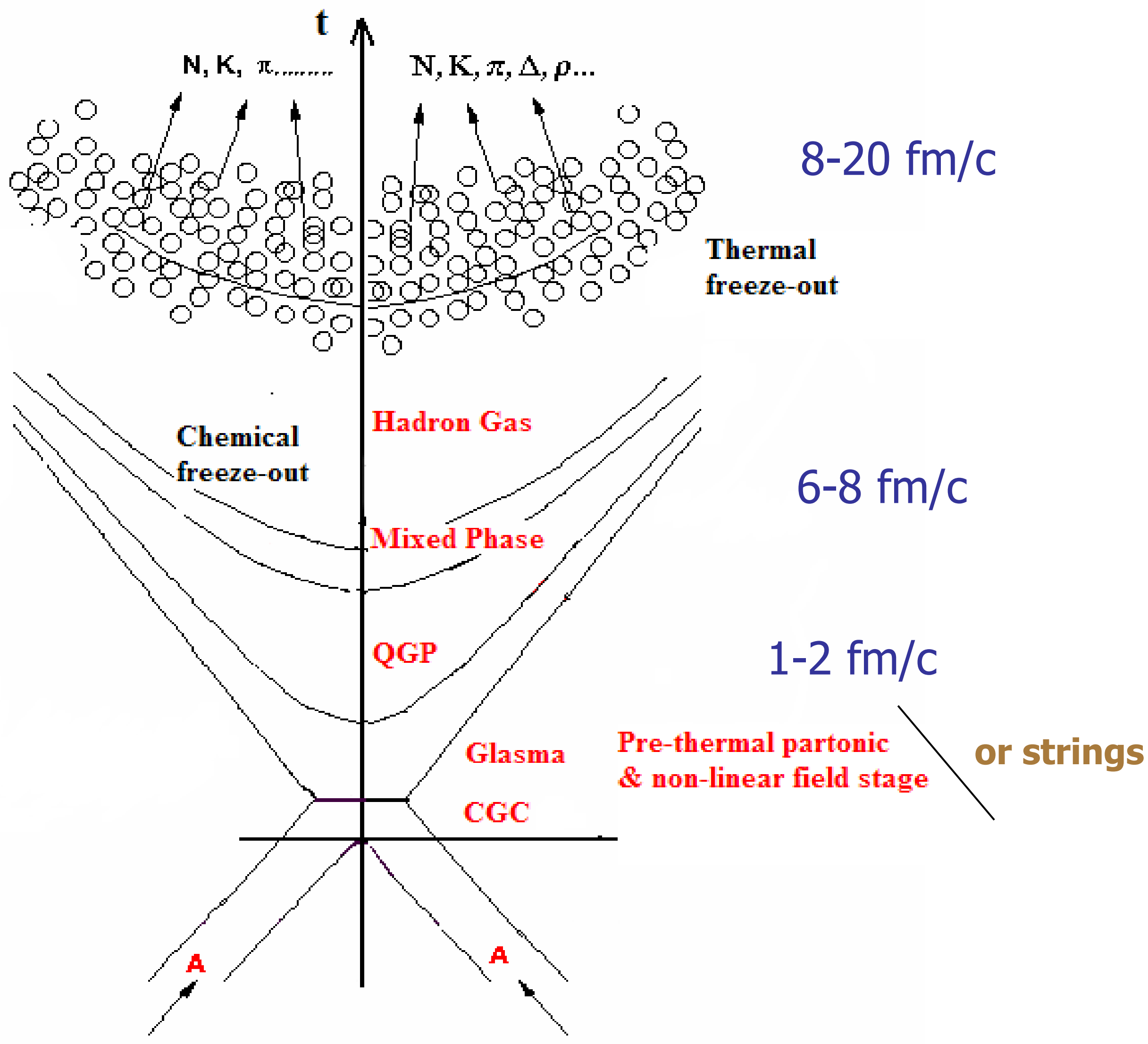

Experimentally discovered thermalization as a great theoretical problem

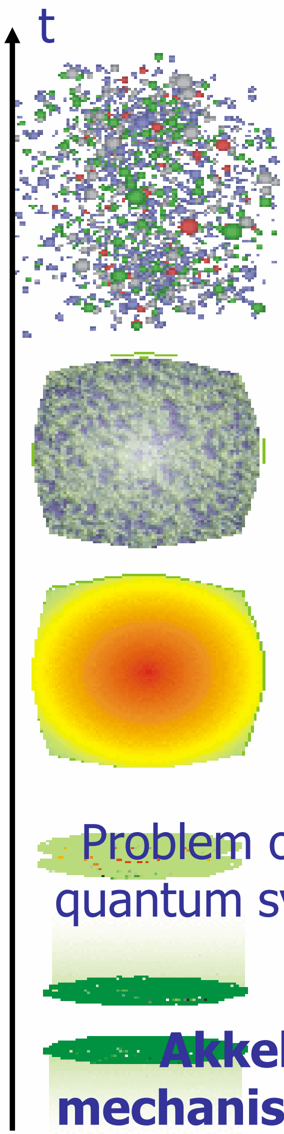

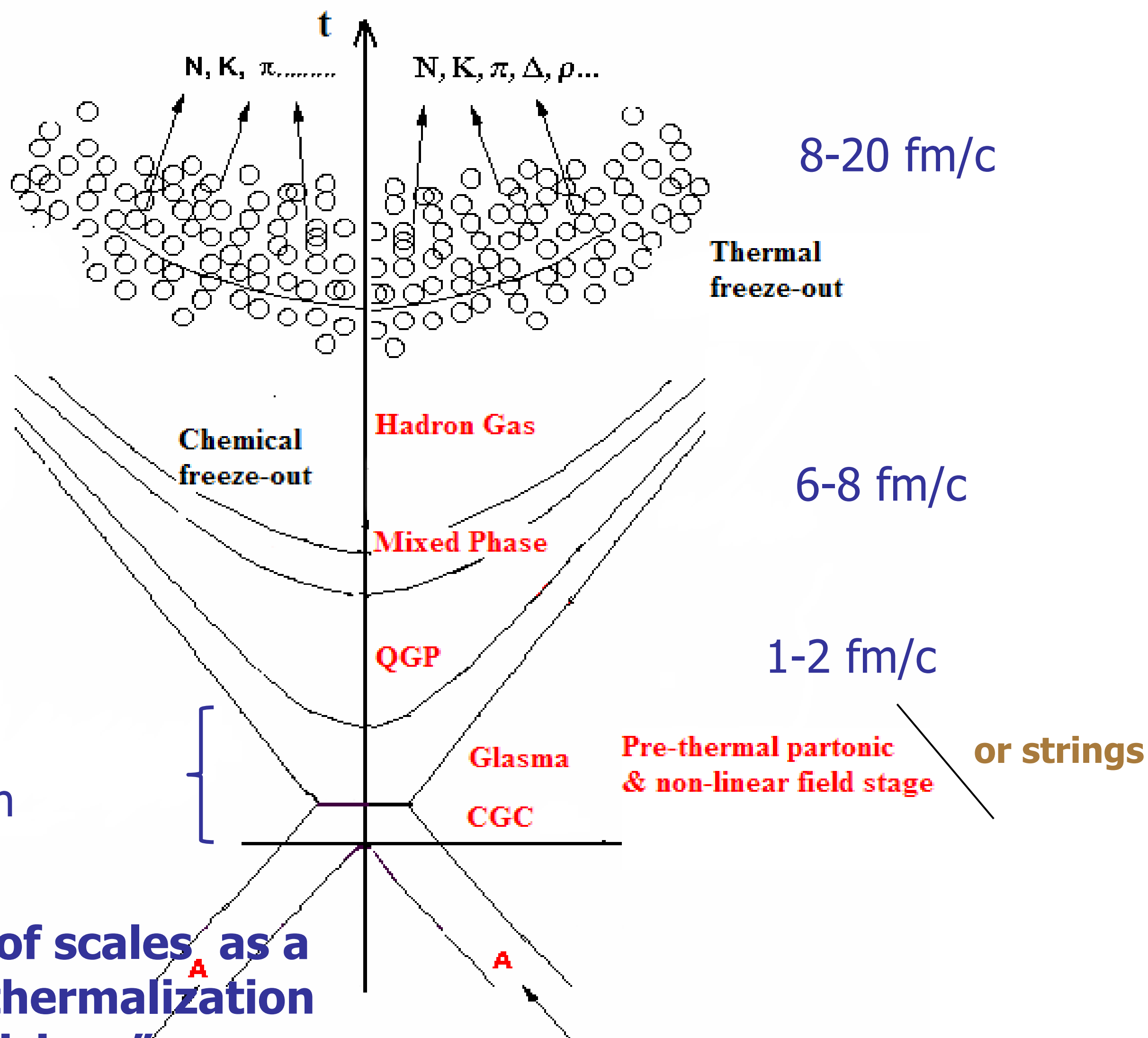

Problem of thermalization for isolated quantum systems with unitary evolution

⇓

Akkelin, Yu.S. "Entanglement of scales as a mechanism for decoherence and thermalization in relativistic heavy ion collisions"

PRC 89 034910 (2014)

Observations and initial and final time scales

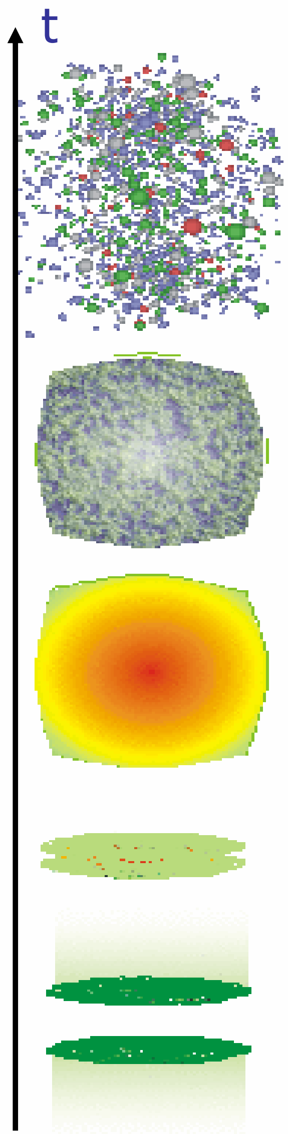

Relatively small space-time scales, $R_{out} / R_{side} \sim 1$ (HBT puzzle)

Early thermal freeze-out: Tth ≈ Tch ≈ 150 MeV

Elliptic flows

Early thermalization at ≈0.5 fm/c

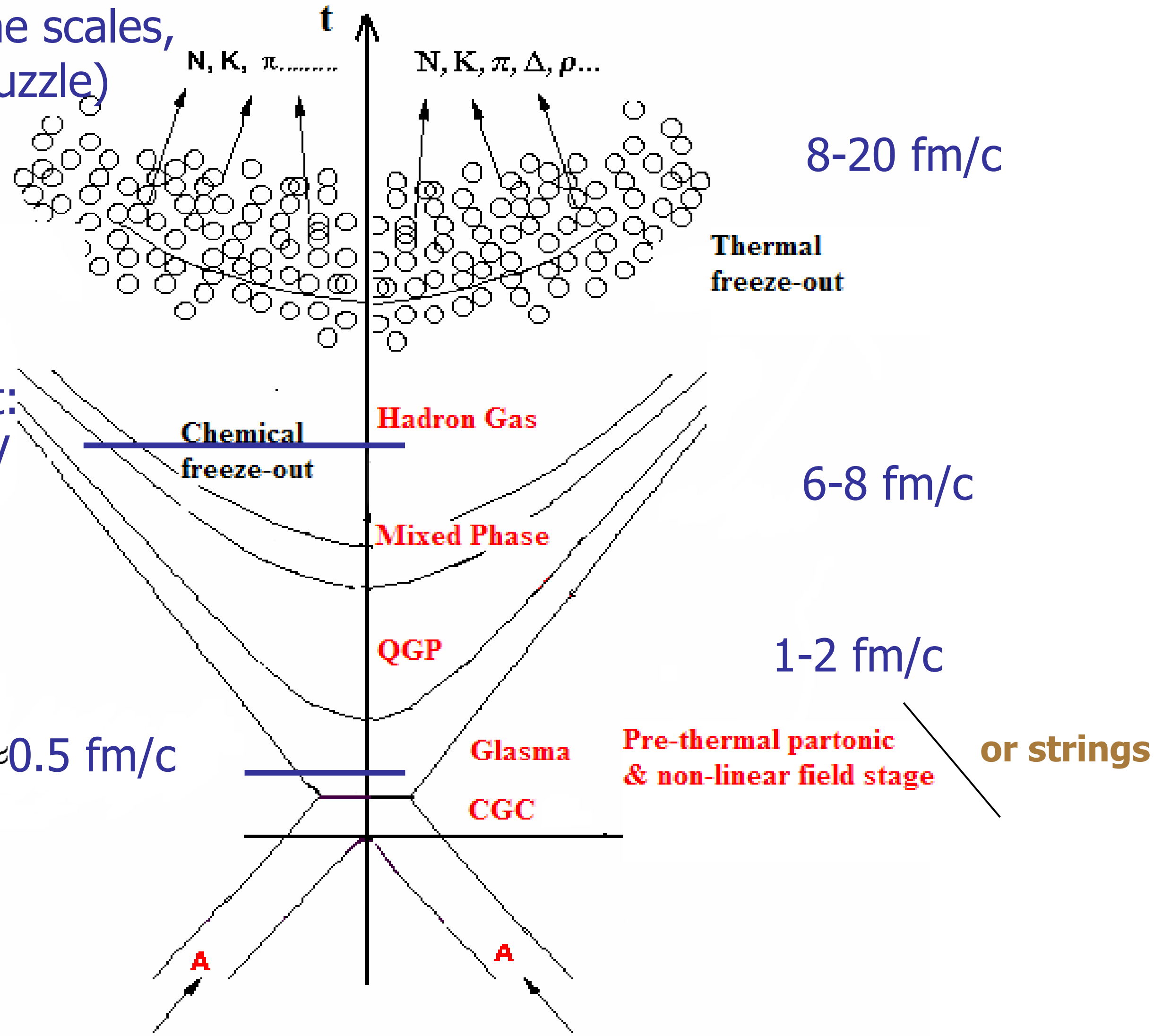

Corrections to the time scales

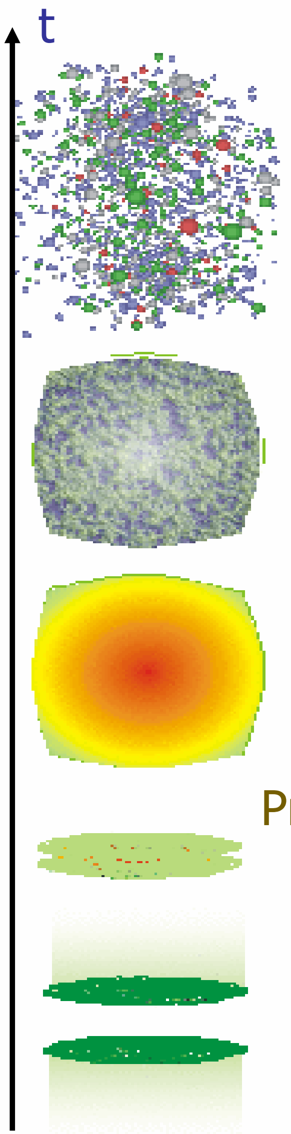

Relatively small space-time scales,
$R_{out} / R_{side} \sim 1$ (HBT puzzle)

↓

HydroKinetic Model (HKM)

↓

No need for early freeze-out

Elliptic flows

↓

Pre-thermal anisotropic transverse flow

↓

No need for very early thermalization (Yu.S. 2006 -2009)

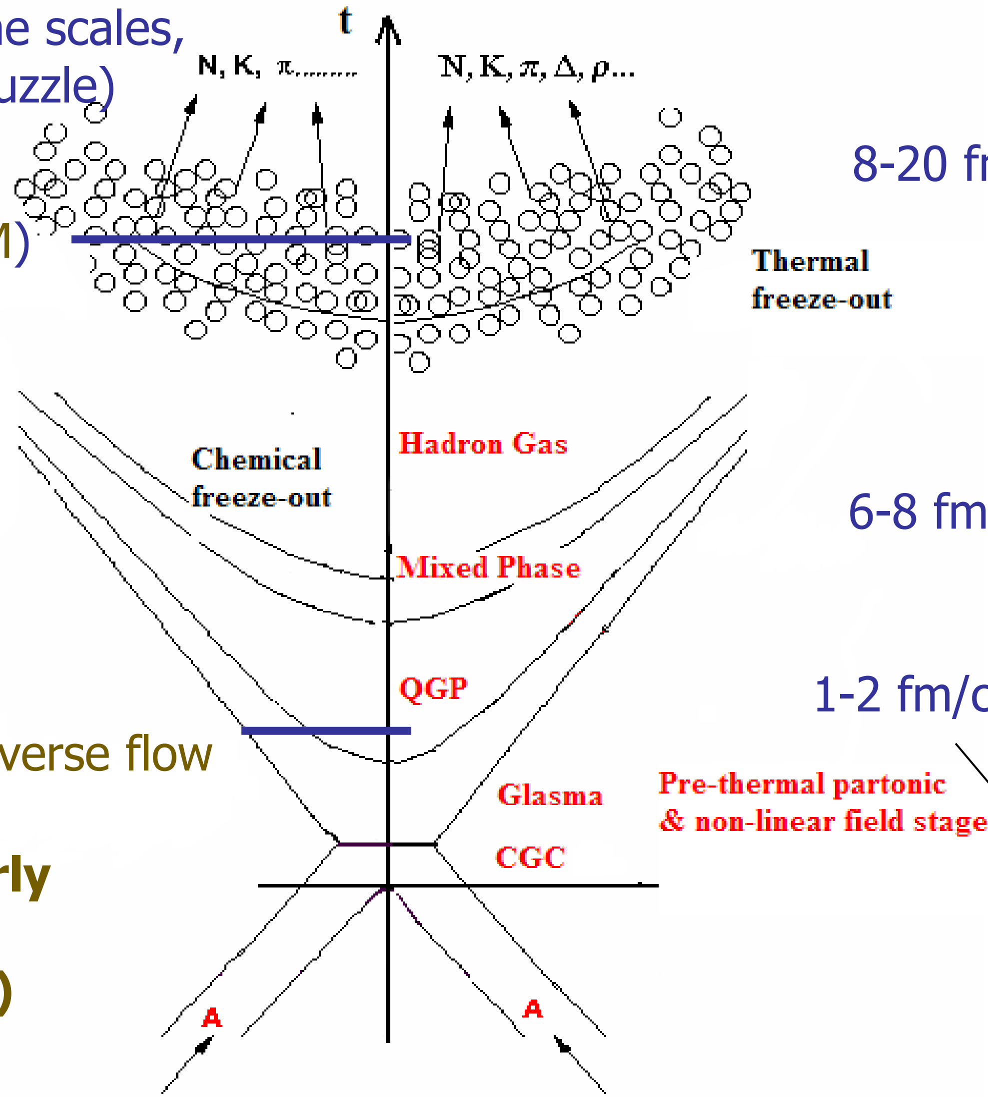

8-20 fm/c

6-8 fm/c

1-2 fm/c

or strings

Further development

Phenomenological model of pre-thermal evolution

Akkelin, Yu.S. , **Matching of nonthermal initial conditions and hydrodynamic stage in ultrarelativistic heavy-ion collisions**
PRC 81, 064901 (2010)

Boltzmann equations and probabilities of particle free propagation

Boltzmann eqs (differential form)

$$\frac{p^\mu}{p^0}\frac{\partial f_i(x,p)}{\partial x^\mu} = G_i(x,p) - L_i(x,p)$$

$G_i(x,p)$ and $L_i(x,p) = R_i(x,p) f_i(x,p)$ are G(ain), L(oss) terms for i p. species

Probability of particle free propagation (for each component i $x = (t, \mathbf{x})$

$$\overline{x}_{t\to s} = (s, \mathbf{x} + \frac{\mathbf{p}}{p^0}(s-t))$$

$$\mathcal{P}_{t\to t'}(x,p) = \exp\left(-\int_t^{t'} ds R(\overline{x}_{t\to s}, p)\right)$$

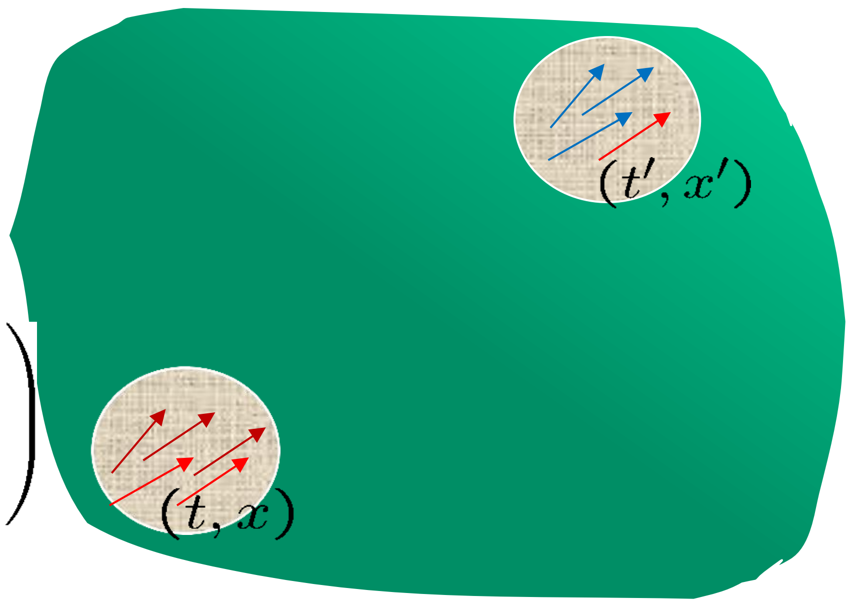

32

Relaxation time approximation

Boltzmann eqs (integral form, Cartesian coord.)

$$f(t,\mathbf{x},p) = f(\overline{x}_{t\to t_0},p)\mathcal{P}_{t_0\to t}(x,p) + \int_{t_0}^{t} G(\overline{x}_{t\to s},p)\mathcal{P}_{s\to t}(x,p)ds$$

$$\overline{x}_{t\to s} = (s,\mathbf{x} - \frac{\mathbf{p}}{p^0}(t-s))$$

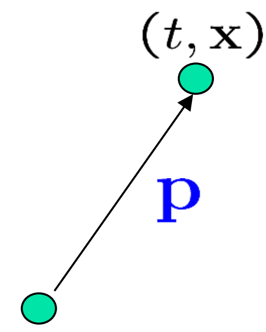

Relaxation time approximation

$$R(x,p) \approx R_{l.eq.} = \frac{1}{\tau_{rel}(x,p)},\ G \approx \frac{f_{l.eq.(x,p)}}{\tau_{rel}(x,p)}$$

Equations in relaxation time approximation

$$\frac{p^\mu}{p_0}\frac{\partial f(x,p)}{\partial x^\mu} = -\frac{f(x,p) - f_{\mathrm{l.eq.}}(x,p)}{\tau_{\mathrm{rel}}(x,p)}$$

in the local rest frame

$$\tau_{\mathrm{rel}}(x,p) = \frac{p_0 \tau^*_{\mathrm{rel}}(x,p)}{p^\mu u_\mu(x)}$$

Basic approach: evolution from τ_0 to τ_{th}

$$\int d^3p \frac{p^\mu p^\nu}{p^0} f(\overline{x}_{\tau\to\tau_0}, p) = T^{\mu\nu}_{free}(x), \qquad \int d^3p \frac{p^\mu p^\nu}{p^0} f_{l.eq.}(\tau, \mathbf{r}, p) = T^{\mu\nu}_{hyd}(x),$$

$$\partial_\mu T^{\mu\nu}_{free}(x) \equiv 0$$

In the approximation: $\mathcal{P}_{\tau_0\to\tau}(x) \approx \mathcal{P}_{\tau_0\to\tau}(\tau)$ and $\frac{\partial f^{\mathrm{l.eq.}}(x,p)}{\partial x^\mu}(1 - \mathcal{P}_{\tau_0\to\tau}(\tau)) \approx 0$

$$T^{\mu\nu}(x) = T^{\mu\nu}_{free}(x)\mathcal{P}_{\tau_0\to\tau}(\tau) + T^{\mu\nu}_{hyd}(x)(1 - \mathcal{P}_{\tau_0\to\tau}(\tau))$$

$$\partial_\mu T^{\mu\nu}(x) = 0 \quad \Rightarrow \quad \begin{aligned} &\partial_\mu \tilde{T}^{\mu\nu}_{hyd}(x) = -T^{\mu\nu}_{free}(x)\partial_\mu \mathcal{P}_{\tau_0\to\tau}(\tau) \\ &\tilde{T}^{\mu\nu}_{hyd} = T^{\mu\nu}_{hyd}(\epsilon \to (1-\mathcal{P}_{\tau_0\to\tau}(\tau))\epsilon, p \to (1-\mathcal{P}_{\tau_0\to\tau}(\tau))p) \end{aligned}$$

Relaxation time. Simple model.

$$\mathcal{P}_{\tau_0\to\tau}(\tau) = \exp\left\{-\int_{\tau_0}^{\tau} \frac{1}{\tau_{\mathrm{rel}}(s)}ds\right\}$$

where $\tau_{\mathrm{rel}}(s) = \tau_{\mathrm{rel}}(\tau_0)\dfrac{\tau_f - s}{\tau_f - \tau_0}$

$$\mathcal{P}_{\tau_0\to\tau}(\tau) = \left(\frac{\tau_f - \tau}{t_f - \tau_0}\right)^{\frac{\tau_f-\tau_0}{\tau_{\mathrm{rel}}(\tau_0)}}$$

$$\mathcal{P}_{\tau_0\to\tau_f}(\tau_0) = 1,\ \mathcal{P}_{\tau_0\to\tau_f}(\tau_f) = 0$$

$$\partial_\mu \mathcal{P}_{\tau_0\to\tau}(\tau)_{|\tau=\tau_f} = 0 \quad \Rightarrow \quad \frac{t_f - t_0}{\tau_{\mathrm{rel}}(t_0)} > 1$$

$$\partial_\mu \tilde{T}^{\mu\nu}_{hyd}(x) = -T^{\mu\nu}_{free}(x)\partial_\mu \mathcal{P}_{\tau_0\to\tau}(\tau) \quad ; \quad \partial_\mu T^{\mu\nu}_{hyd}(x) = 0 \text{ at } t \geq t_f$$

Viscous hydrodynamics

$$\partial_{;\mu}\widetilde{T}^{\mu\nu}_{\mathtt{hyd}}(x) = -T^{\mu\nu}_{\mathtt{free}}(x)\partial_{;\mu}\mathcal{P}(\tau) \qquad \widetilde{T} = T(1-\mathcal{P}(\tau))$$

$$(1-\mathcal{P}(\tau))\left\langle u^\gamma \partial_{;\gamma}\frac{\widetilde{\pi}^{\mu\nu}}{(1-\mathcal{P}(\tau))}\right\rangle = -\frac{\widetilde{\pi}^{\mu\nu}-(1-\mathcal{P}(\tau))\pi^{\mu\nu}_{\mathtt{NS}}}{\tau_\pi} - \frac{4}{3}\widetilde{\pi}^{\mu\nu}\partial_{;\gamma}u^\gamma$$

The boost invariant initial distribution function for free streaming in LCMS

$$f(x,p) = g\exp\left(-\sqrt{\frac{p_T^2}{\lambda_\perp^2}+\frac{p_L^2}{\lambda_\parallel^2}}\right)\rho(\mathbf{r}_T) \qquad \lambda \equiv \lambda_\perp/\lambda_\parallel = 1 \text{ or } 100$$

$$\rho(\mathbf{r}_T) = \exp(-r_x^2/R_x^2 - r_y^2/R_y^2)$$

or taken from MC Glauber IC

$$\tau_0 = 0.1 \text{ fm/c},\ \tau_f = 1 \text{ fm/c}$$

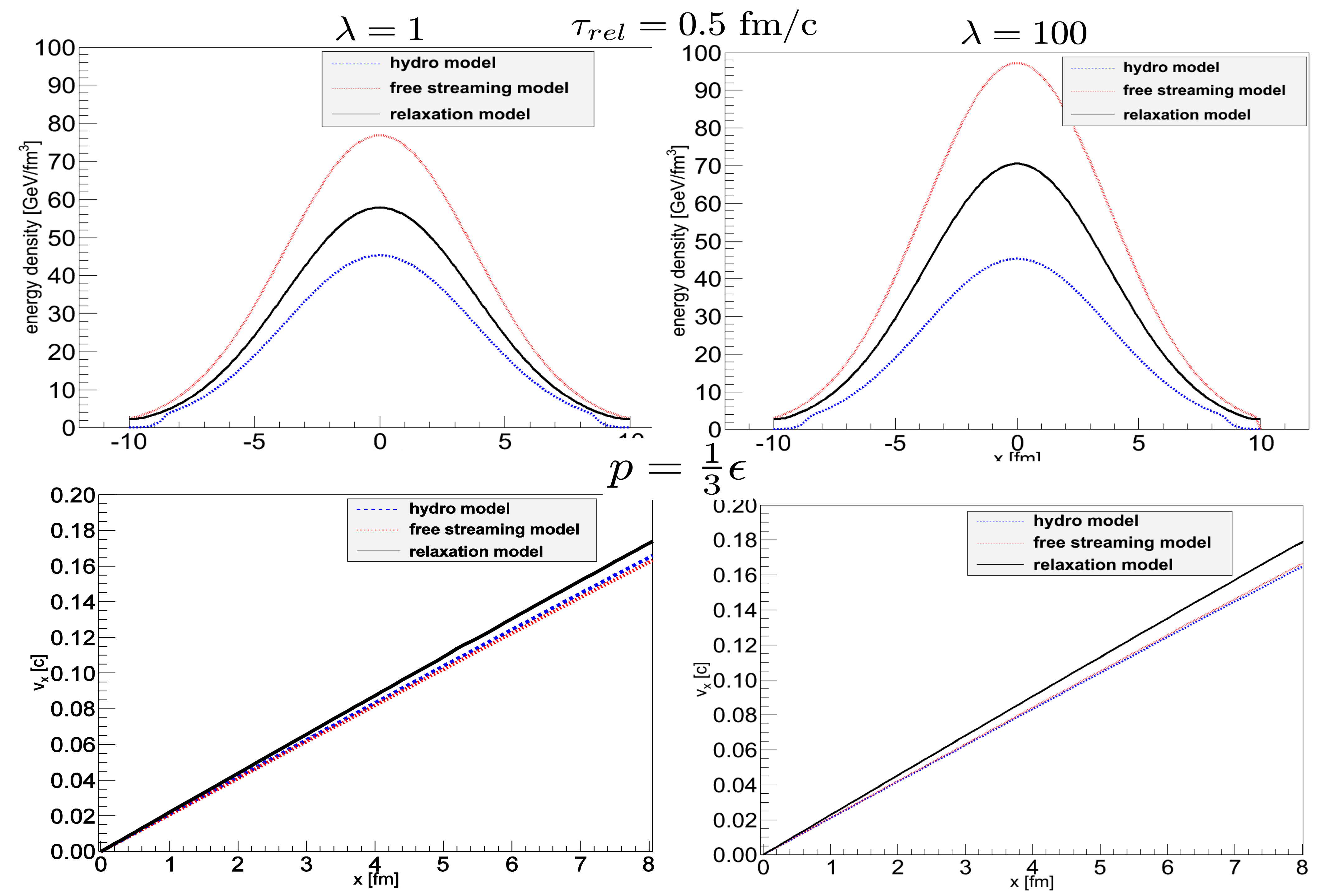

λ = 1
τ_rel = 0.5 fm/c
λ = 100
p = 1/3 ε
hydro model
free streaming model
relaxation model
energy density [GeV/fm^3]
v_x [c]
x [fm]

Viscous hydro

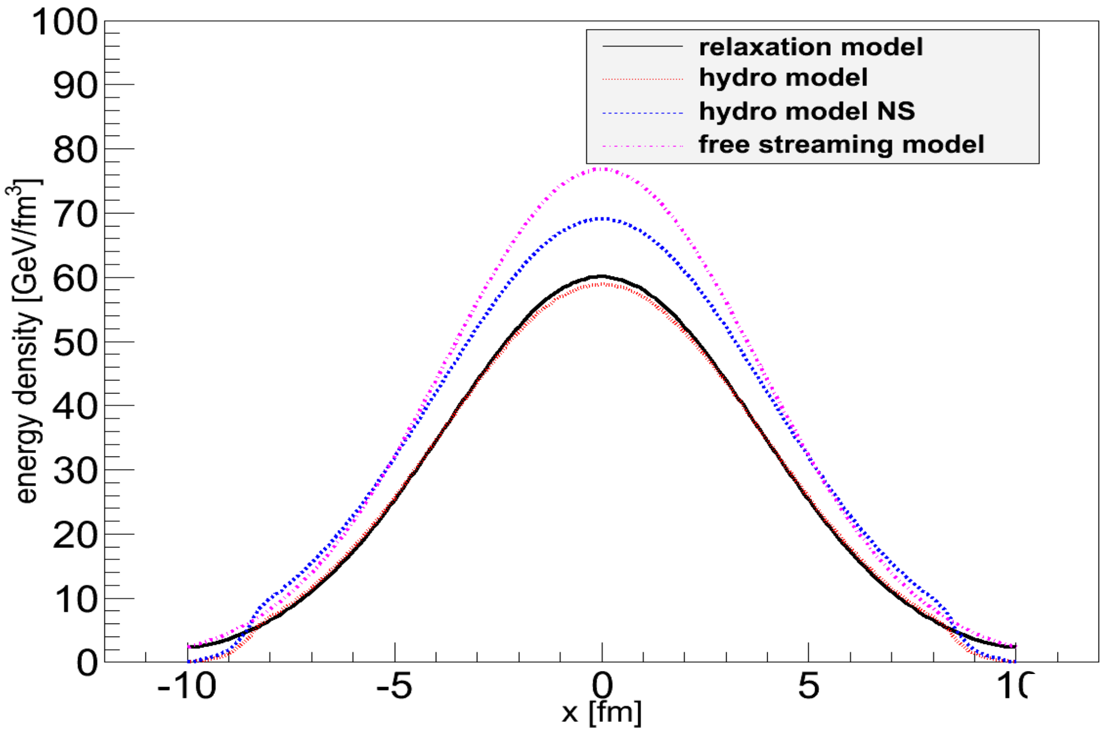

$$p = \frac{1}{3}\epsilon$$

$$\lambda = 1$$

$$\tau_{rel} = 0.5 \text{ fm/c}$$

$$\frac{\eta}{s} = 0.2$$

$$p = \frac{1}{3}\epsilon$$

$$\lambda = 1$$

$$\tau_{rel} = 0.5 \text{ fm/c}$$

$$\frac{\eta}{s} = 0.2$$

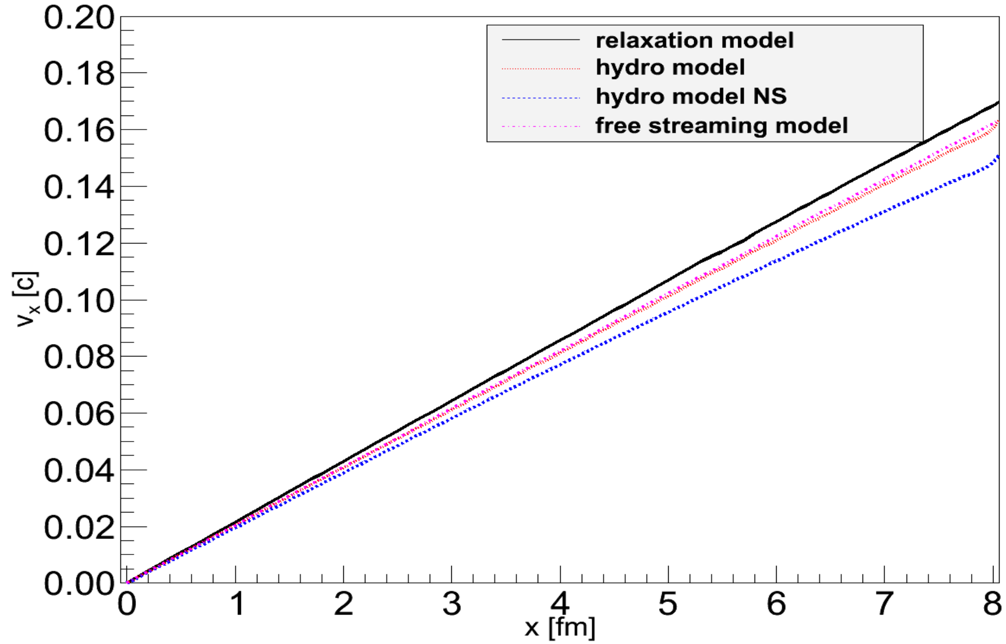

Summary

- **If some model (effective QCD approach) gives us the energy-momentum tensor at time τ_0 , one can estimate the flows and energy densities at expected time of thermalization τ_{th} using equations for fluid with (known) source terms.**

- **This phenomenological approach is motivated by Boltzmann equations, it accounts for the energy and momentum conservation laws and contains the three parameters: initial time of the energy density formation τ_0 , supposed time of thermalization τ_{th} and relaxation time τ_{rel} .**

***

- **In the case if the target energy-momentum tensor corresponds to viscous fluid,**

the model is easily generalized for viscous hydro.

Important is that the relaxation model can be applied to any initial conditions that provide e-by-e analysis. It is in contrast with so-called "anisotropic hydrodynamics".

The stages of the matter evolution in A+A collisions

The initial huge kinetic energy of colliding nuclei converts into masses of the final observed particles (several tens of thousands) + the energy of collective flow

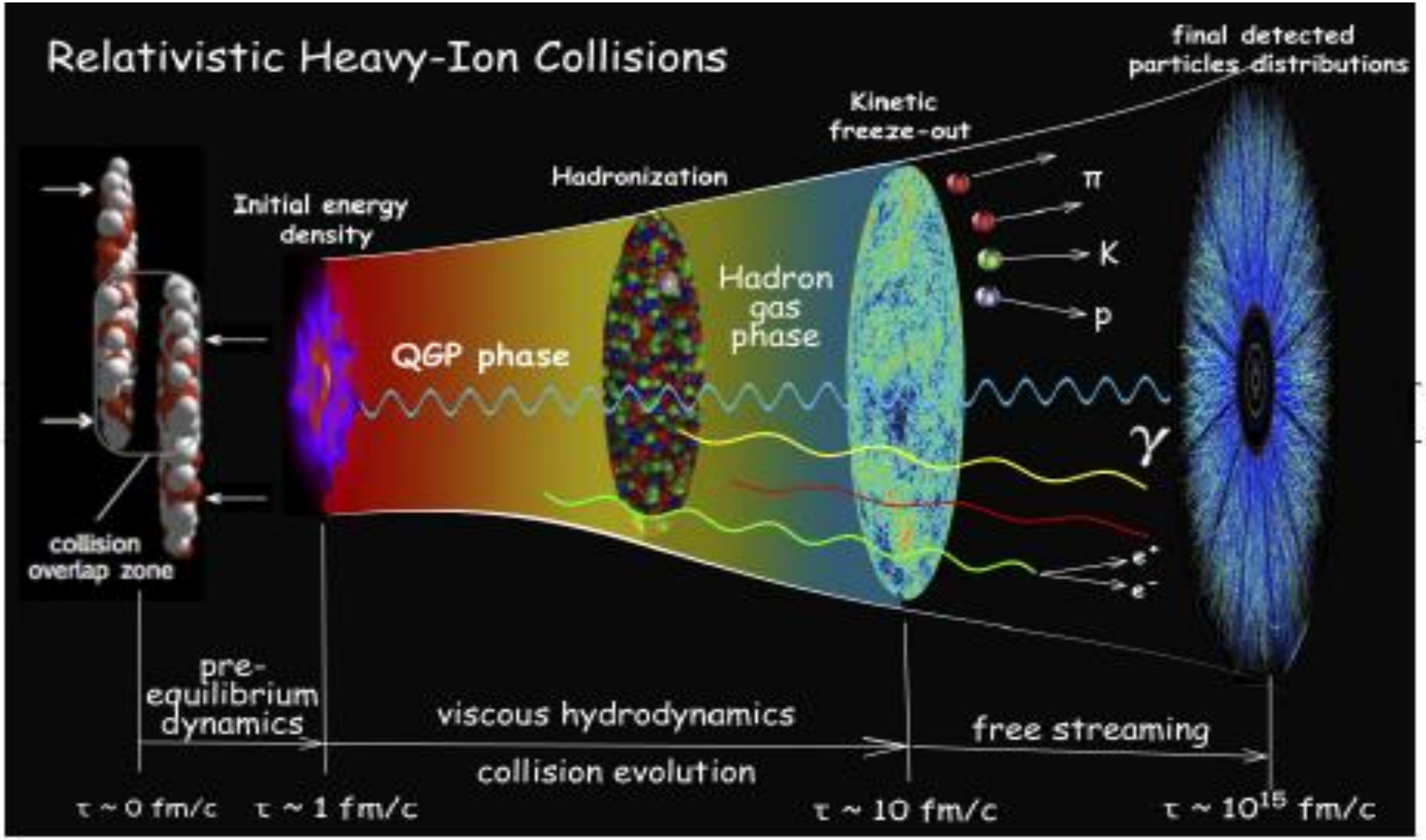

Integrated HydroKinetic model: HKM $\longrightarrow$ iHKM

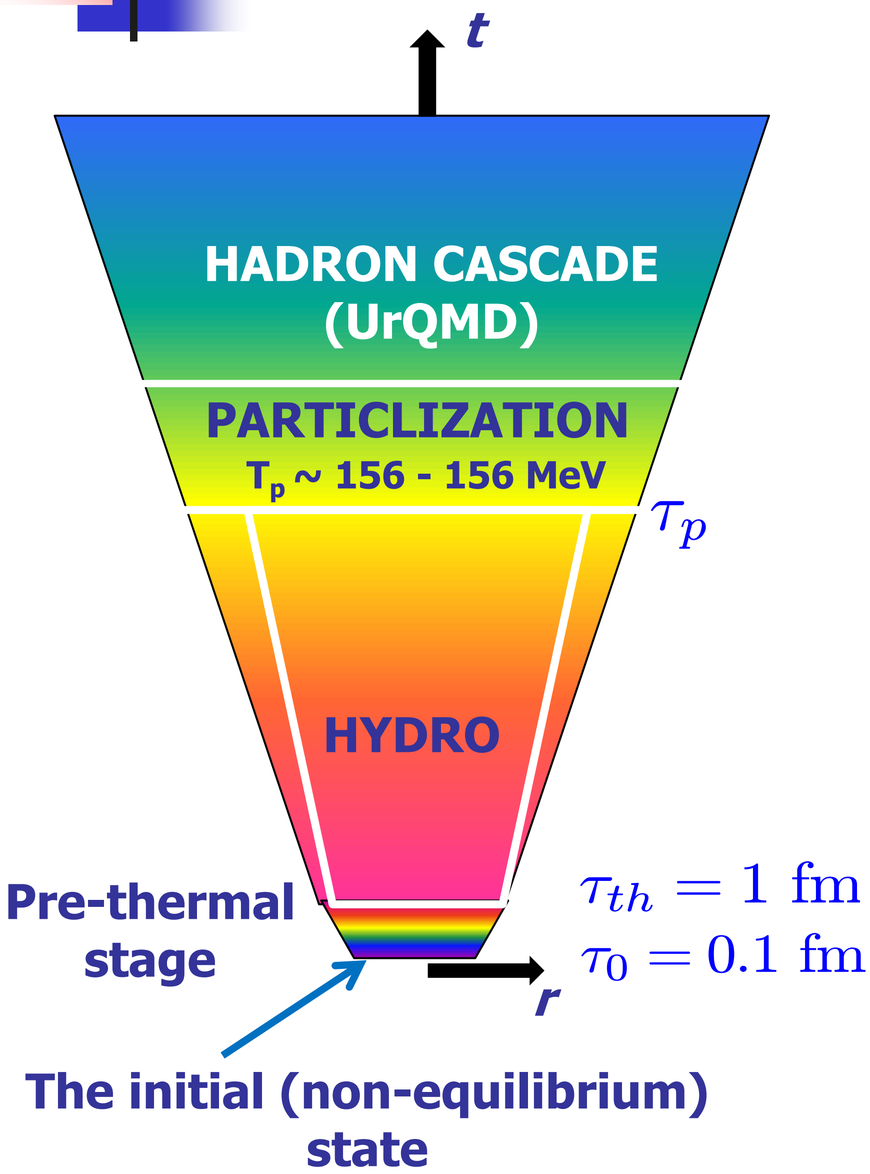

Complete algorithm incorporates the stages:

- **generation of the initial states;**
- **thermalization of initially non-thermal matter;**
- **viscous chemically equilibrated hydrodynamic expansion;**
- **sudden (with option: continuous) particlization of expanding medium;**
- **a switch to UrQMD cascade with near equilibrium hadron gas as input;**
- **simulation of observables.**

Yu.S., Akkelin, Hama: PRL 89 (2002) 052301;
... + Karpenko: PRC 78 (2008) 034906;
Karpenko, Yu.S. : PRC 81 (2010) 054903;
... PLB 688 (2010) 50;
Akkelin, Yu.S. : PRC 81 (2010) 064901;
Karpenko, Yu.S., Werner: PRC 87 (2013) 024914;
Naboka, Akkelin, Karpenko, Yu.S. : PRC 91 (2015) 014906;
Naboka, Karpenko, Yu.S. Phys. Rev. C 93 (2016) 024902.

.

Initial flows and Ro/Rs ratio (t_0=1-2 fm/c)

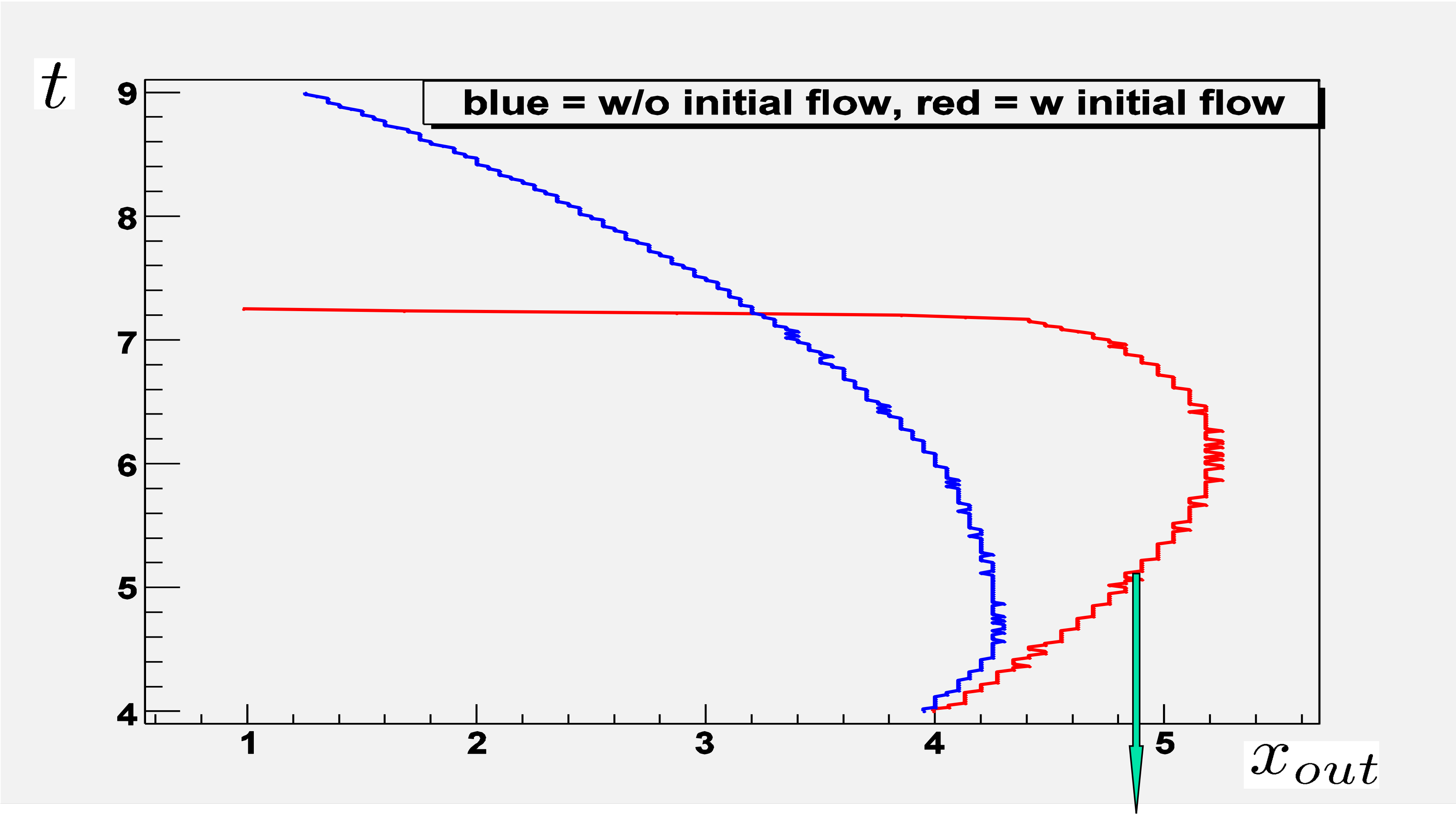

$$R_{out}^2 \approx R_{side}^2 + v^2 \langle \triangle t^2 \rangle_p - 2v \langle \triangle x_{out} \triangle t \rangle_p, v = \frac{p_T}{p^0}$$

Emission functions for top SPS, RHIC and LHC energies

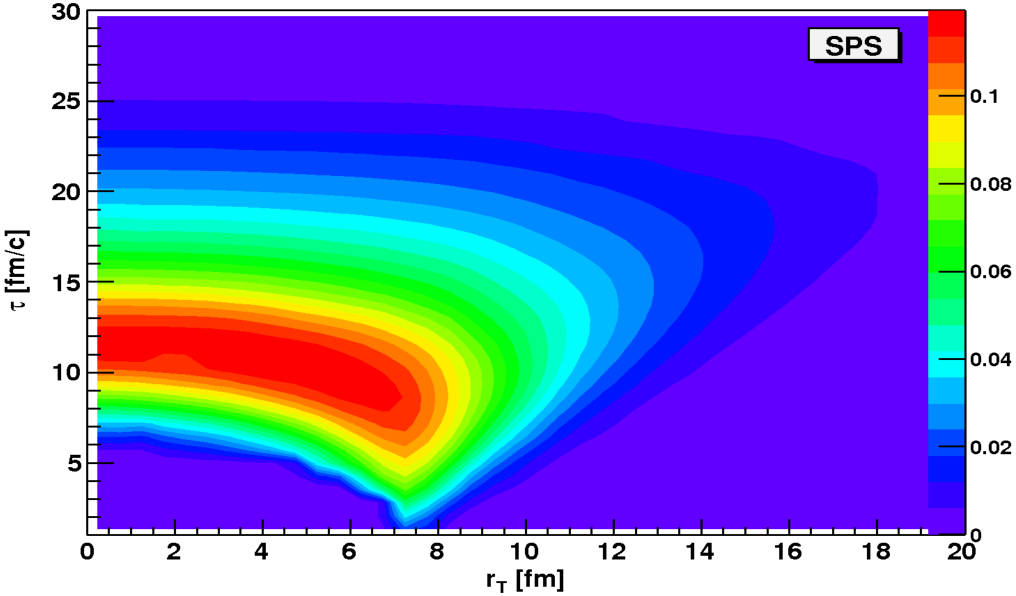

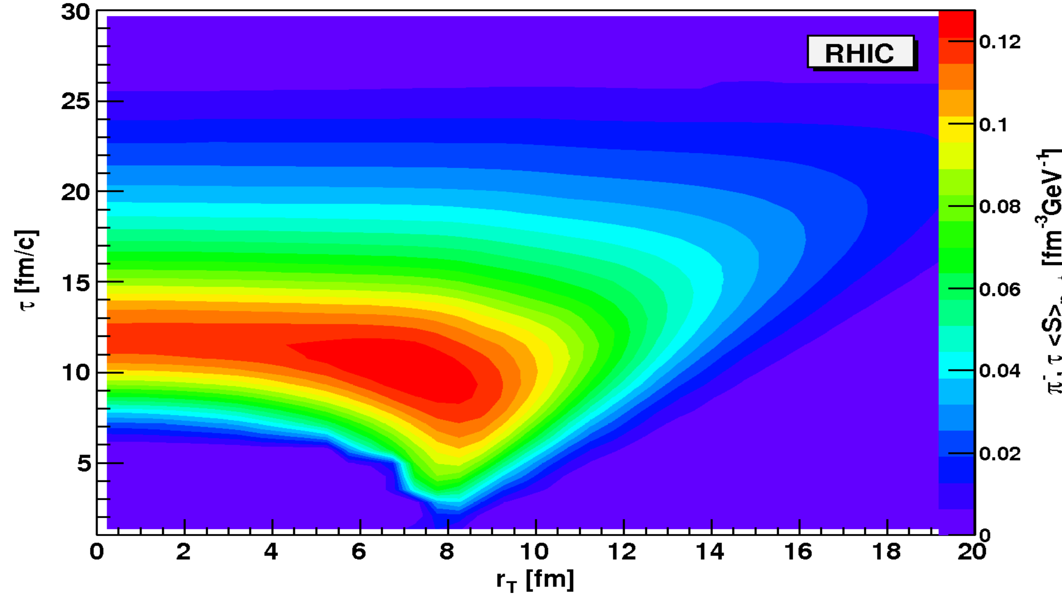

$$R_{out}^2 \approx R_{side}^2 + v^2\langle \triangle t^2\rangle_p - 2v\langle \triangle x_{out}\triangle t\rangle_p, v = \frac{p_T}{p^0}$$

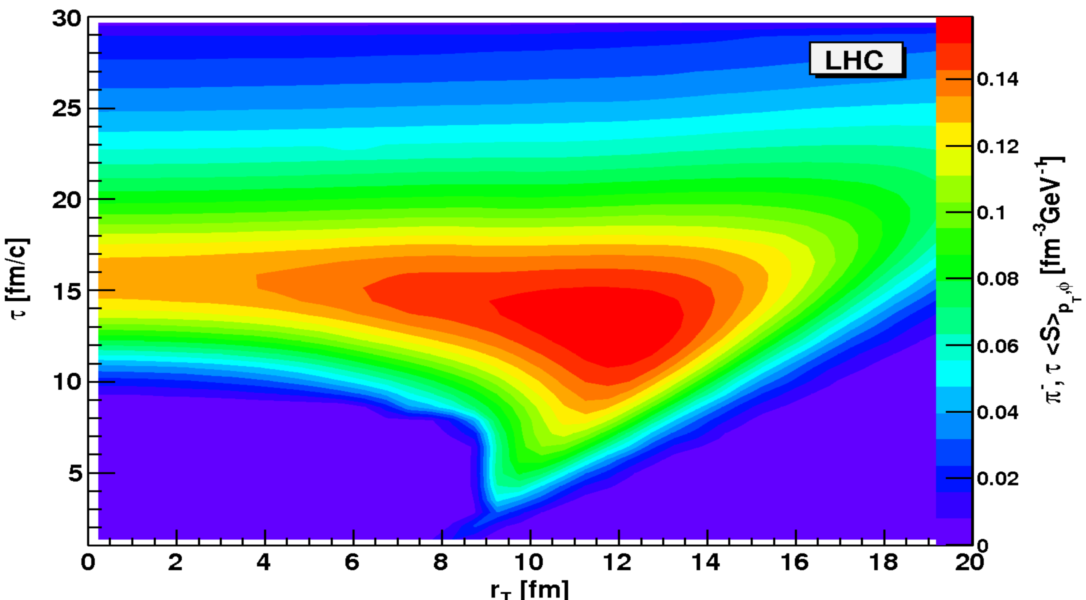

HKM prediction: solution of the HBT Puzzle

Two-pion Bose–Einstein correlations in central Pb–Pb collisions at $\sqrt{s_{NN}} = 2.76$ TeV ☆ ALICE Collaboration Physics Letters B 696 (2011) 328-

ALICE

Quotations:

Available model predictions are compared to the experimental data in Figs. 2-d and 3. Calculations from three models incorporating a hydrodynamic approach, AZHYDRO [45], KRAKOW [46,47], and HKM [48,49], and from the hadronic-kinematics-based model HRM [50,51] are shown. An in-depth discussion is beyond the scope of this Letter but we notice that, while the increase of the radii between RHIC and the LHC is roughly reproduced by all four calculations, only two of them (KRAKOW and HKM) are able to describe the experimental R_{out}/R_{side} ratio.

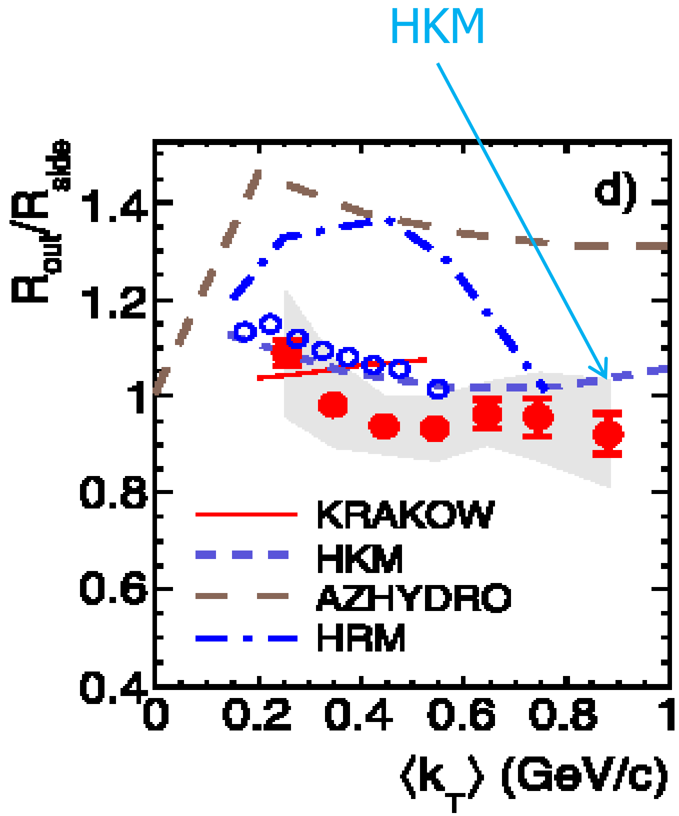

[48] I.A. Karpenko, Y.M. Sinyukov, Phys. Lett. B 688 (2010) 50.
[49] N. Armesto, et al. (Eds.), J. Phys. G 35 (2008) 054001.

Interferometry volume Vint in LHC p-p and **central** Au-Au, Pb-Pb collisions

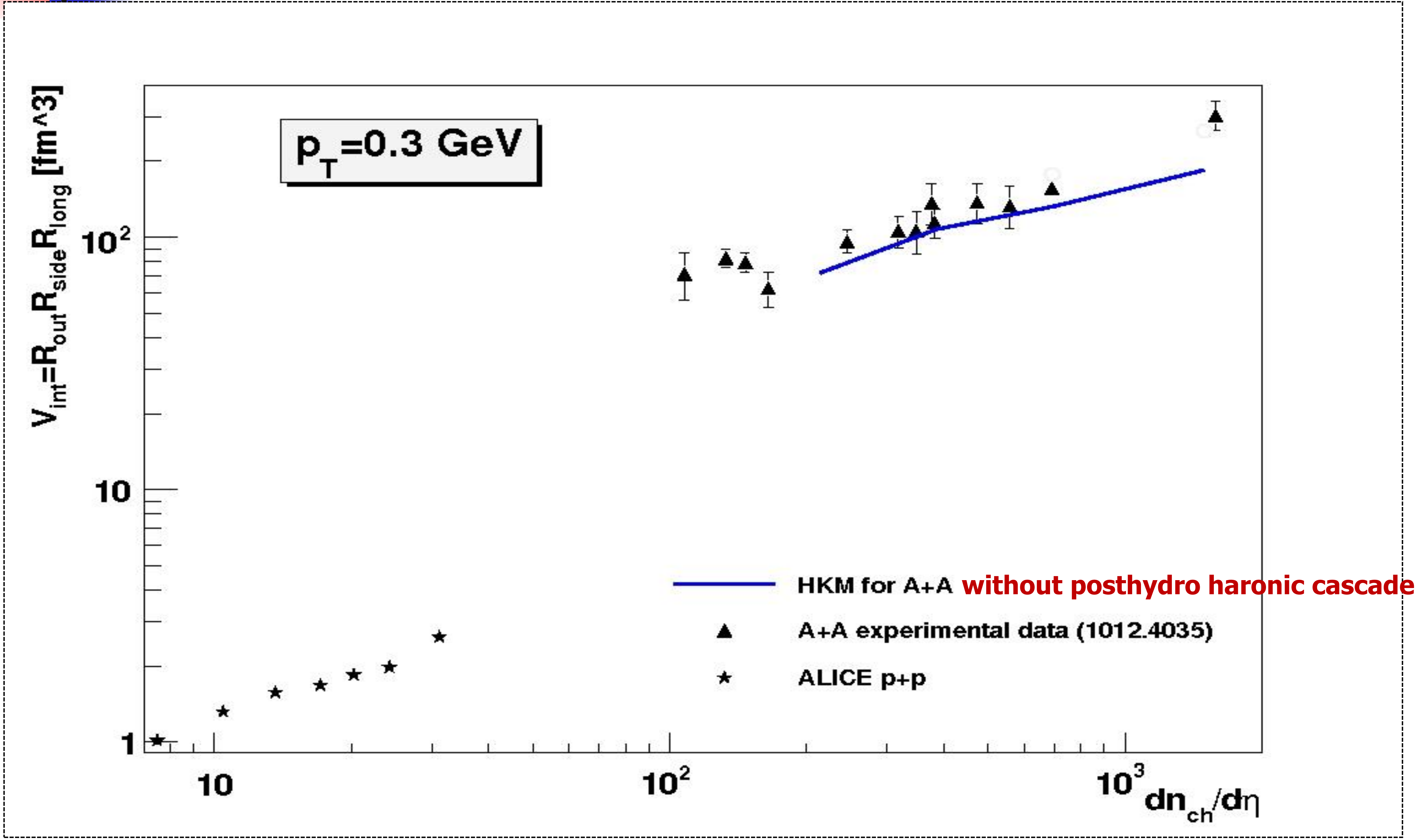

Interferometry volume Vint in LHC p-p and **central** Au-Au, Pb-Pb collisions

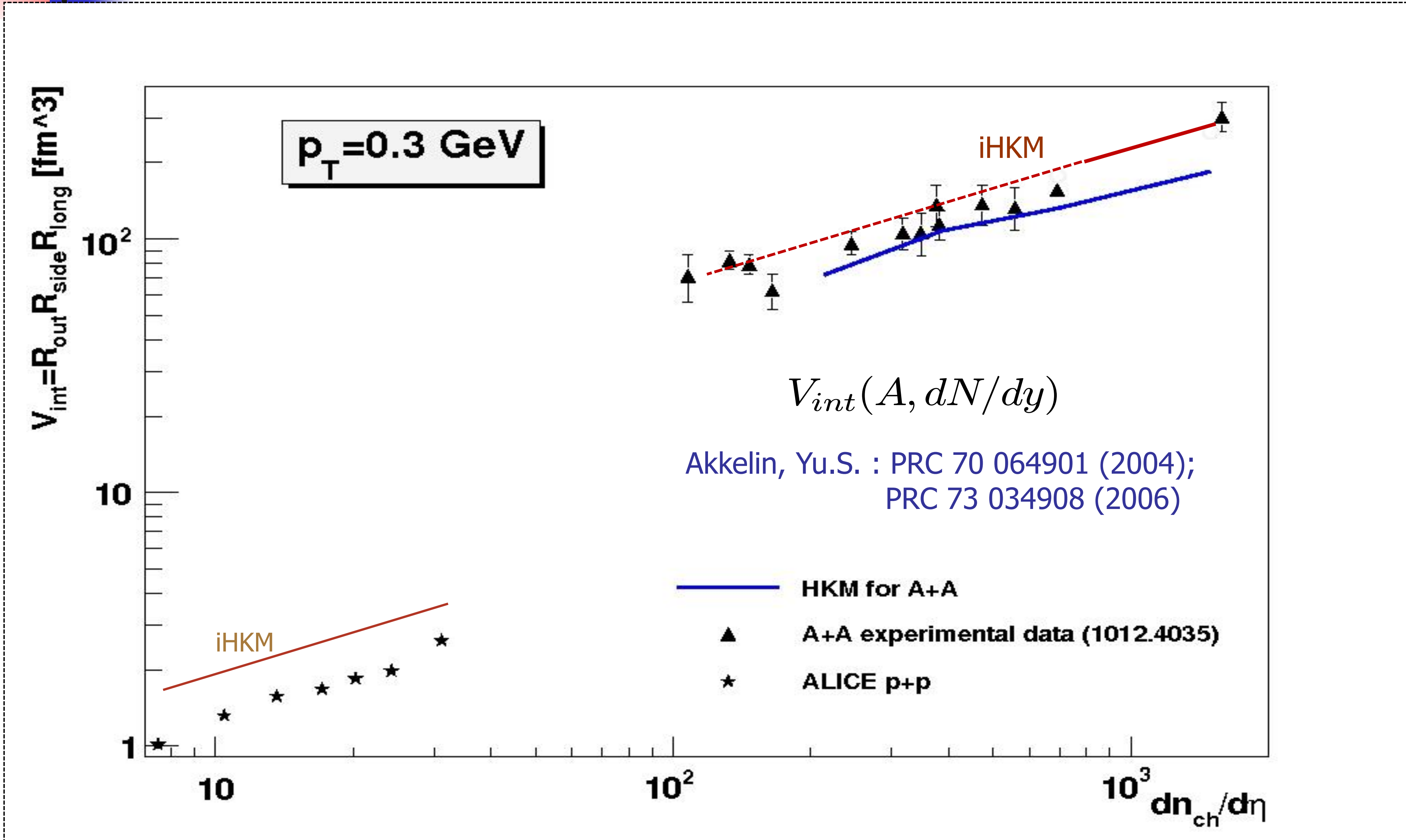

Interferometry volume Vint in LHC p-p and **central** Au-Au, Pb-Pb collisions

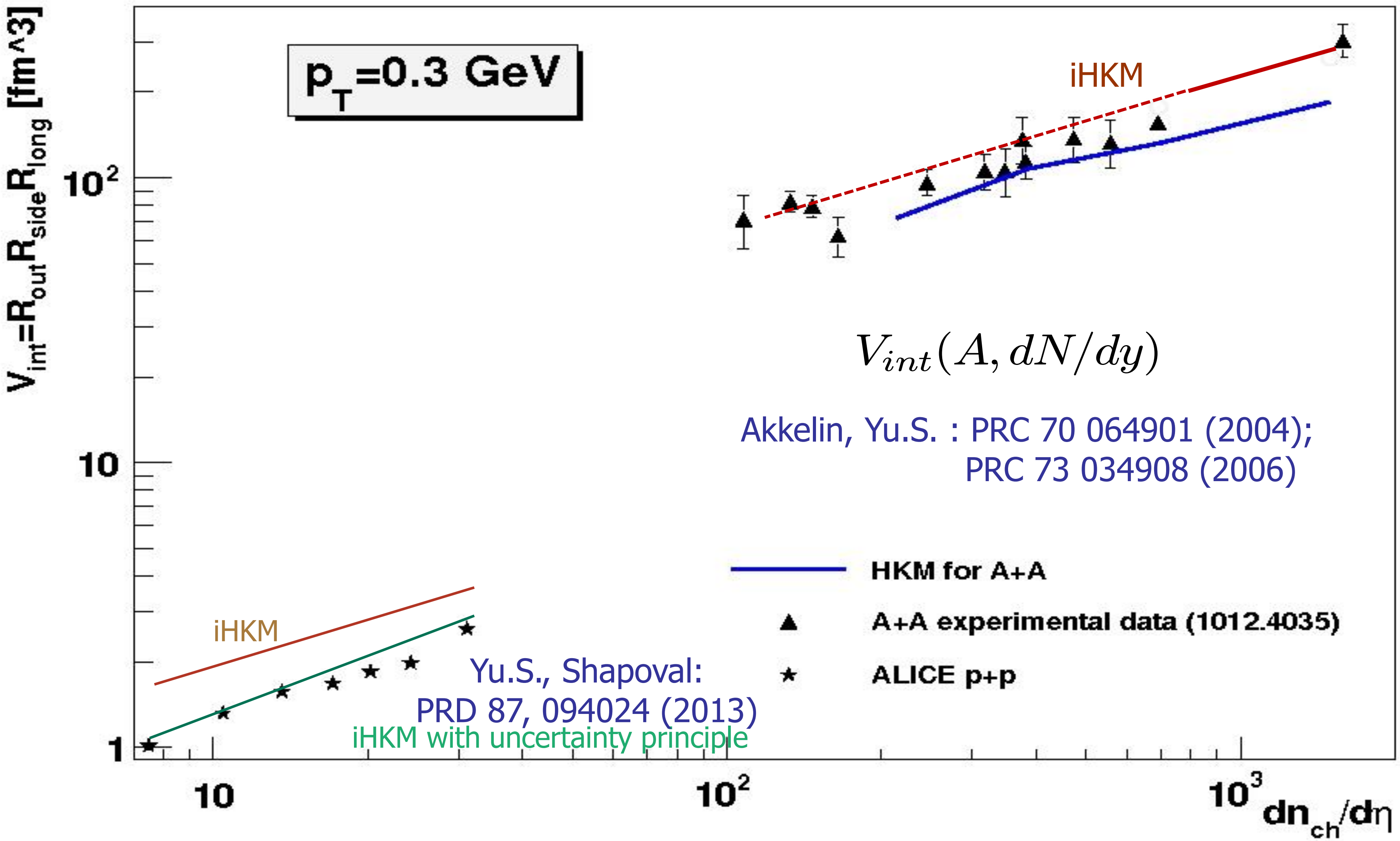

Interferometry volume Vint in LHC p-p and **central** Au-Au, Pb-Pb collisions

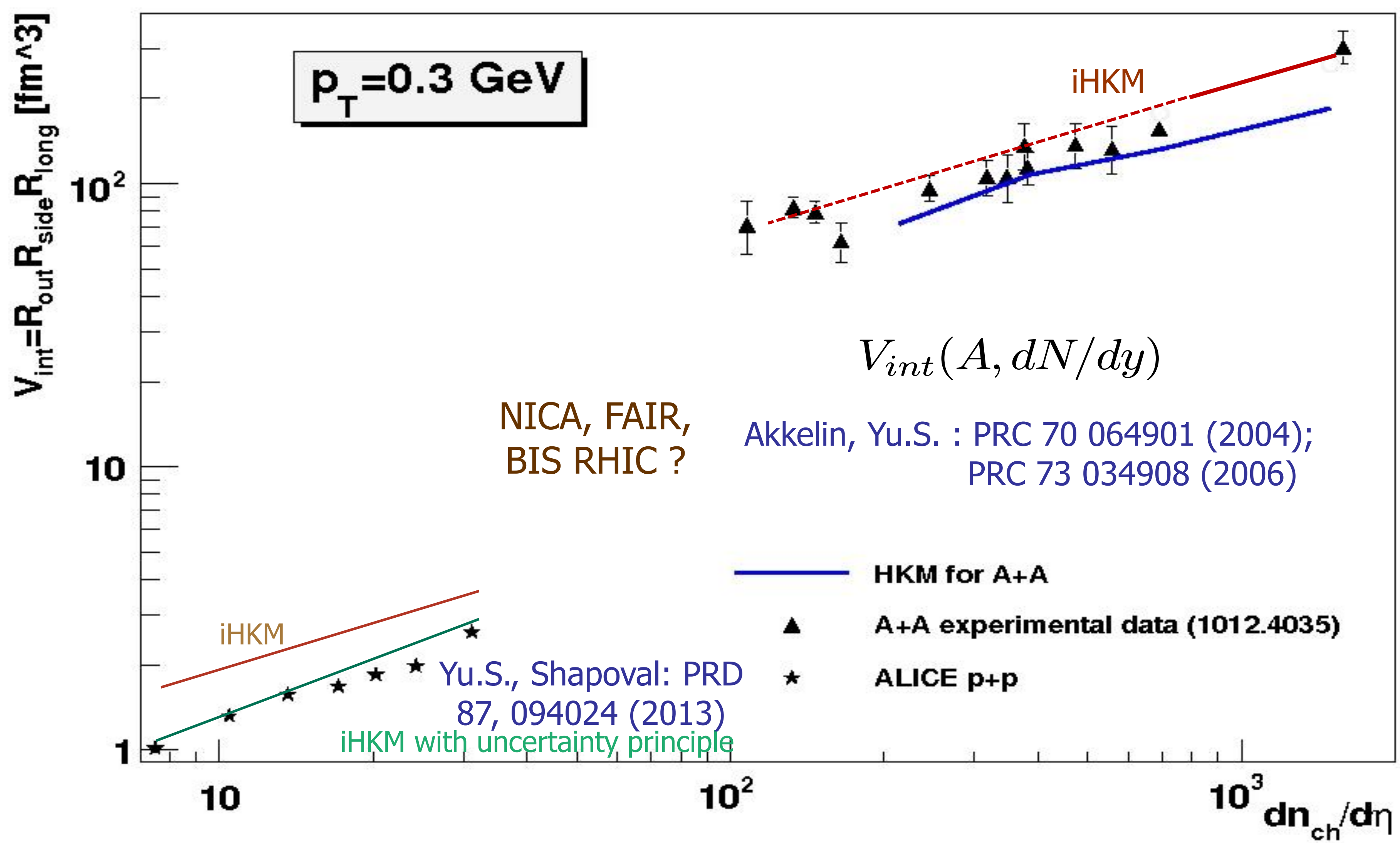

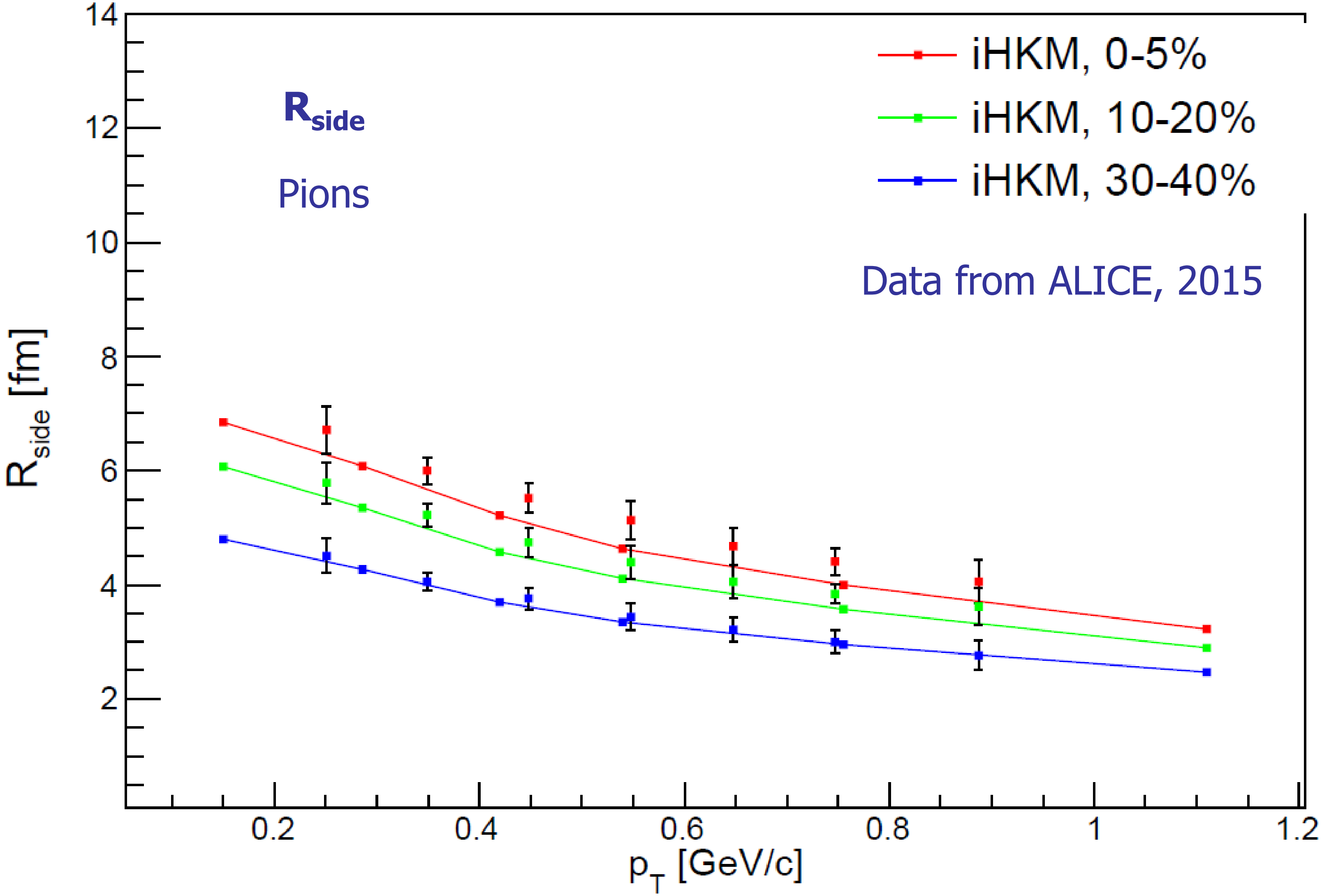

The R_{side} dependence on transverse momentum for different centralities in the iHKM scenario under the same conditions as in Fig. 1. The experimental data are from [33].

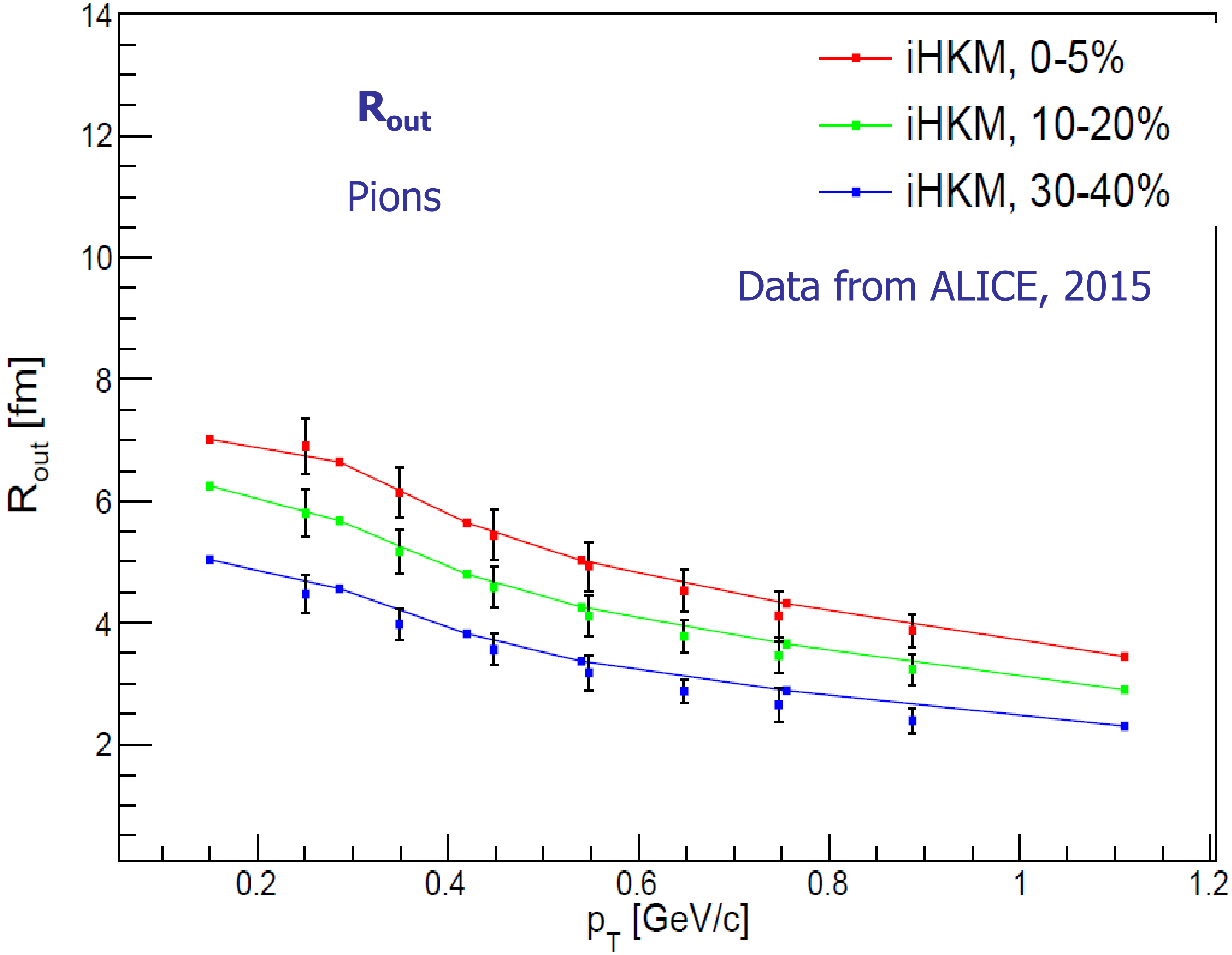

The R_{out} dependence on transverse momentum for different centralities in the iHKM basic scenario under the same conditions as in Fig. 1.

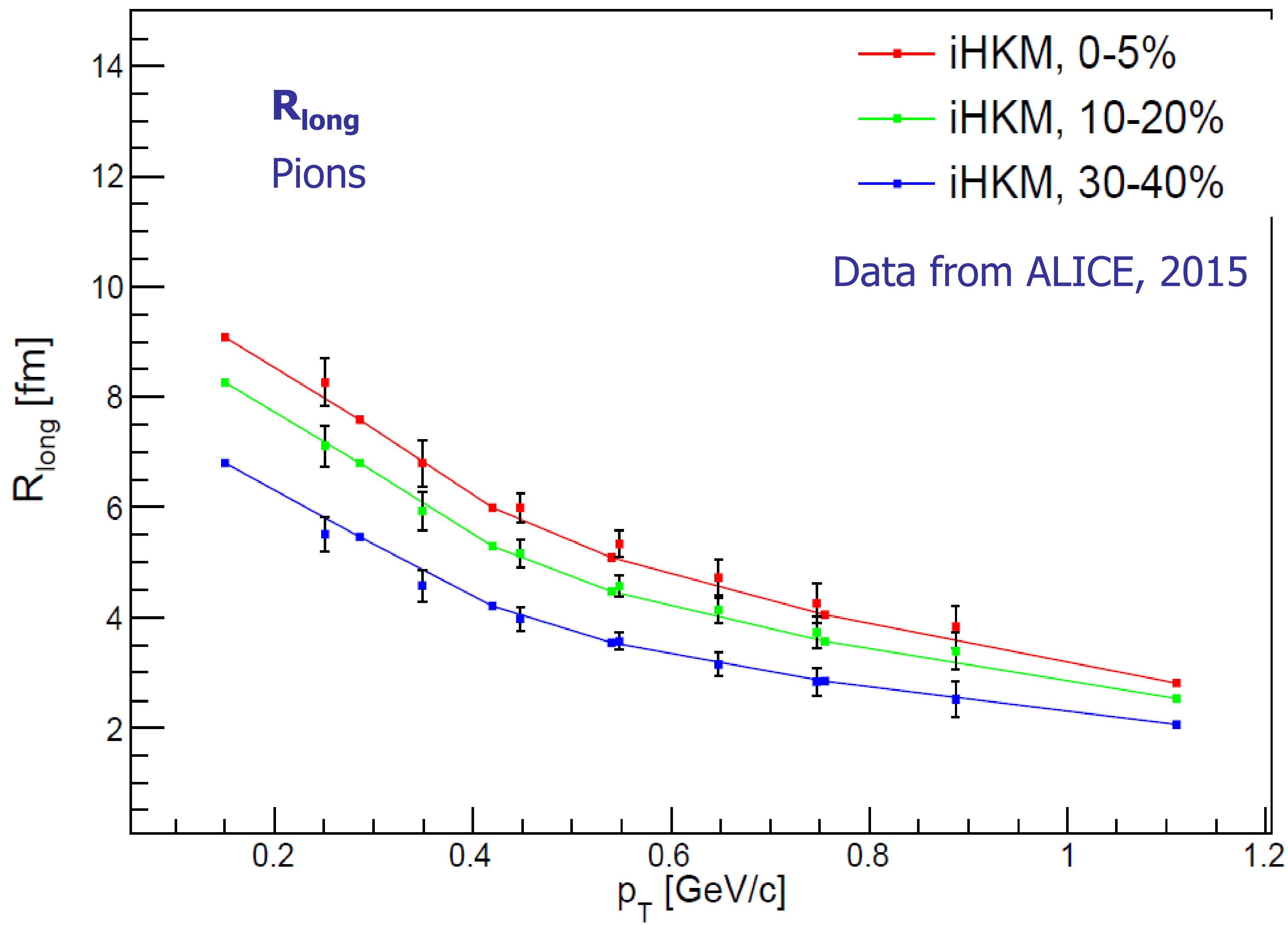

The R_{long} dependence on transverse momentum for different centralities in the iHKM basic scenario - the same conditions as in Fig. 1. The experimental data are from [33].

HKM predictions for kaon femtoscopy

Freeze-out Dynamics via Charged Kaon Femtoscopy in $\sqrt{s_{NN}}$=200 GeV Central Au+Au Collisions

STAR Collaboration

arXiv:1302.3168 February 2013

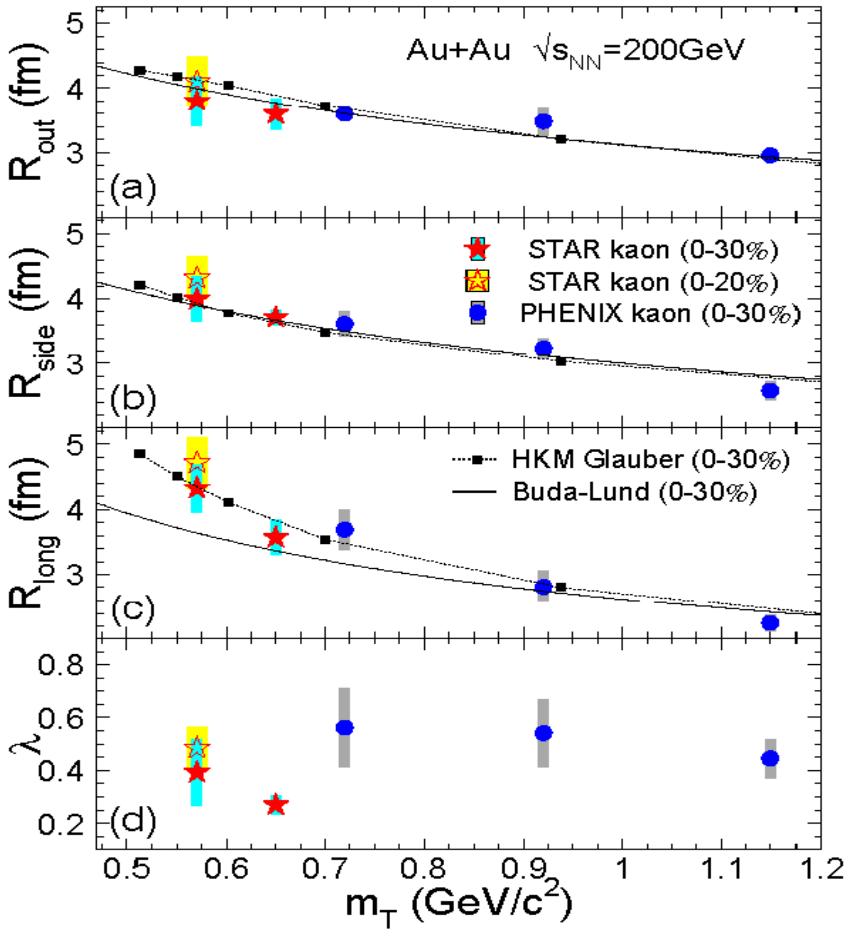

FIG. 4. Transverse mass dependence of Gaussian radii (a) R_{out}, (b) R_{side} and (c) R_{long} for mid-rapidity kaon pairs from the 30% most central Au+Au collisions at $\sqrt{s_{NN}}$=200 GeV. STAR data are shown as solid stars; PHENIX data [10] as solid circles (error bars include both statistical and systematic uncertainties). Hydro-kinetic model [23] with initial Glauber condition and Buda-Lund model [22] calculations are shown by solid squares and solid curves, respectively.

Quotations:

Our measurement at $0.2 \le k_T \le 0.36$ GeV/c clearly favours the HKM model as more representative of the expansion dynamics of the fireball.

....

In the outward and sideward directions, this decrease is adequately described by m_T–scaling. However, in the longitudinal direction, the scaling is broken. The results are in favor of the hydro-kinetic predictions [23] over pure hydrodynamical model calculations.

....

[23] I. A. Karpenko and Y. M. Sinyukov, Phys. Rev. C **81** (2010) 054903.

Extraction of the fireball life time from long. femto scale

$$\underbrace{R_l^2(k_T) = \tau^2\lambda^2\left(1+\frac{3}{2}\lambda^2\right)}_{2015} \approx \text{w/o transv. expansion} \approx \underbrace{\tau^2\frac{T}{m_T}}_{1987}\underbrace{\frac{K_2(\frac{m_T}{T})}{K_1(\frac{m_T}{T})}}_{1995} \quad m_T\text{-scaling}$$

where

$$\lambda^2 = \frac{T}{m_T}\left(1 - \overbrace{\frac{k_T^2}{(m_T+\alpha T)^2}}^{\bar{v}_T^2}\right)^{1/2}$$

Yu.S., Shapoval, Naboka, Nucl. Phys. A 946 (2016) 247 (arXiv:1508.01812)

$K^{\pm}K^{\pm}$ and $K^0_s K^0_s$ in Pb-Pb: HKM model

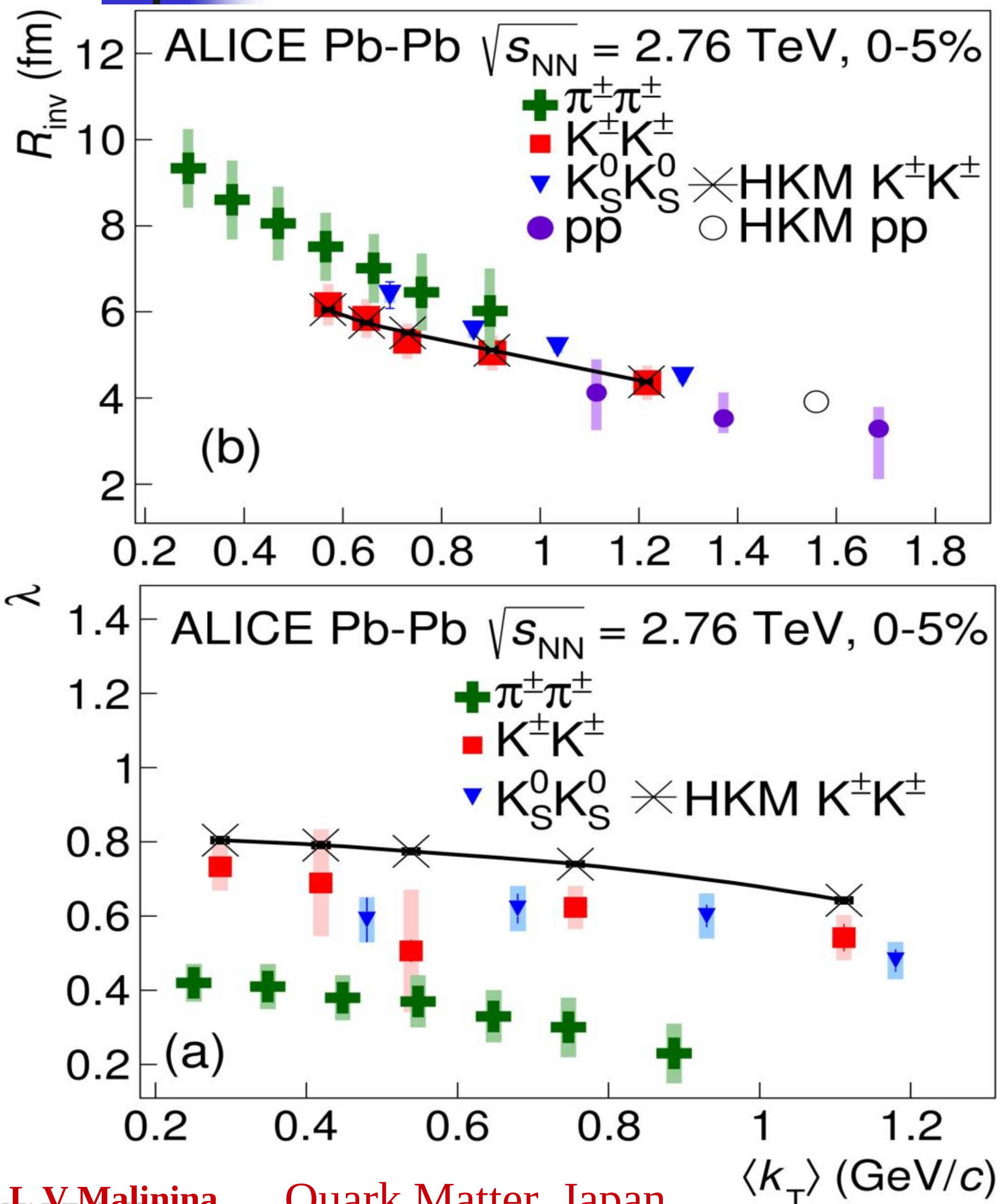

New results from ArXiv.org:1506.07884

- R and λ for $\pi^{\pm}\pi^{\pm}$, $K^{\pm}K^{\pm}$, $K^0_s K^0_s$, pp for 0-5% centrality
- Radii for kaons show good agreement with HKM predictions for $K^{\pm}K^{\pm}$
  (V. Shapoval, P. Braun-Munzinger, Yu. Sinyukov Nucl.Phys.A929 (2014))

- λ decrease with k_T, both data and HKM
- HKM prediction for λ slightly overpredicts the data
- Λ_{π} are lower λ_K due to the stronger influence of resonances

ALICE Coll. arXiv:1709.01731 (PRC, 2017)

Comparison with HKM for 0-5% centrality

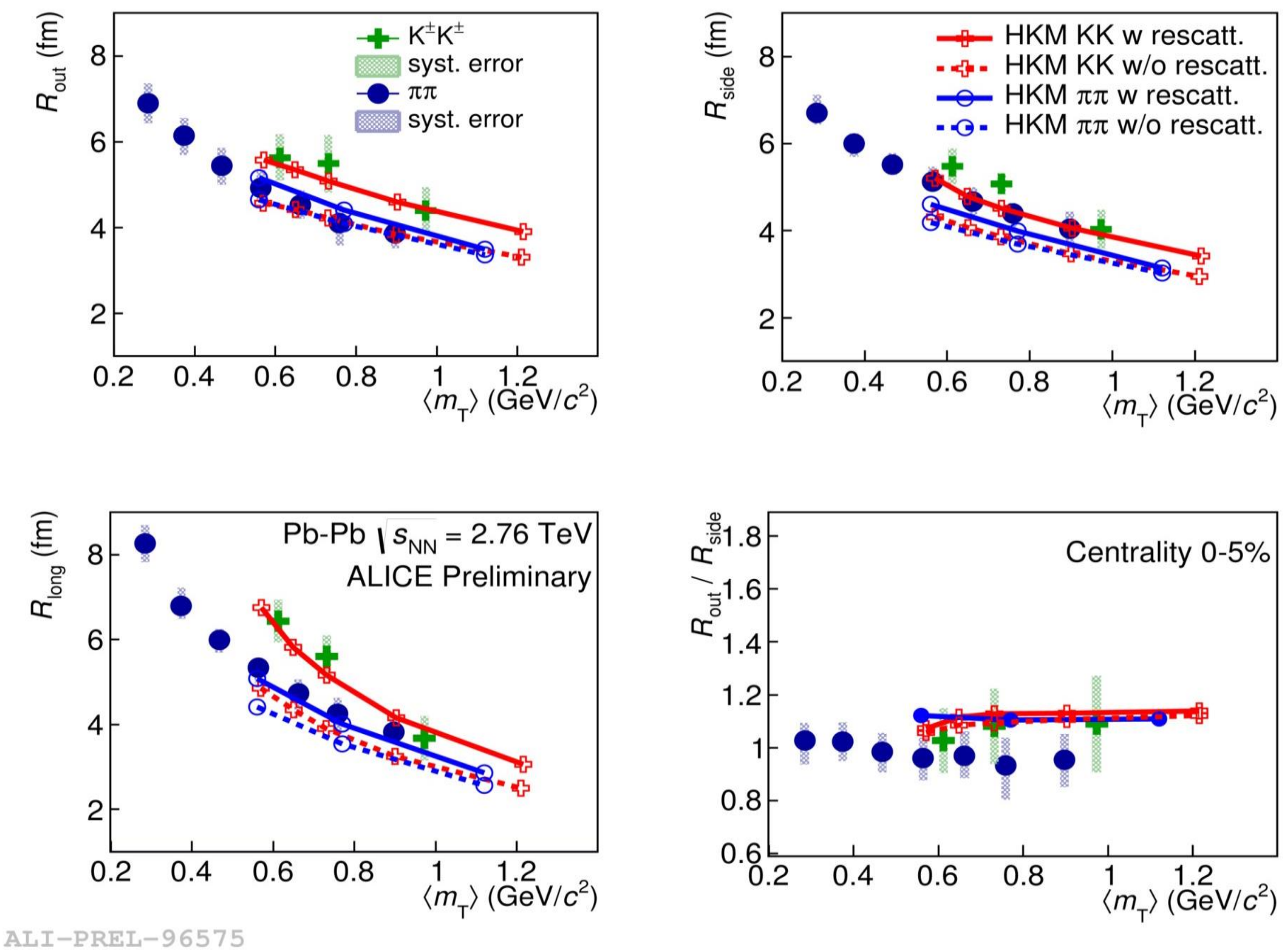

- HKM model with re- scatterings (M. Shapoval, P. Braun-Munzinger, Iu.A. Karpenko, Yu.M. Sinyukov, Nucl.Phys. A 929 (2014) 1.) describes well ALICE π & K data.

- HKM model w/o re-scatterings demonstrates approximate m_T scaling

  for π & K, but does not describe ALICE π & K data

- The observed deviation from m_T scaling is explained in (M. Shapoval, P. Braun-Munzinger, Iu.A. Karpenko, Yu.M. Sinyukov, Nucl.Phys. A 929 (2014) by essential transverse flow & re-scattering phase.

- HKM model slightly underestimates R_{side} overestimates *R_side /R_out*

3D K±K± & ππ radii versus k_T

Pion results from ArXiv.org:1507.06842

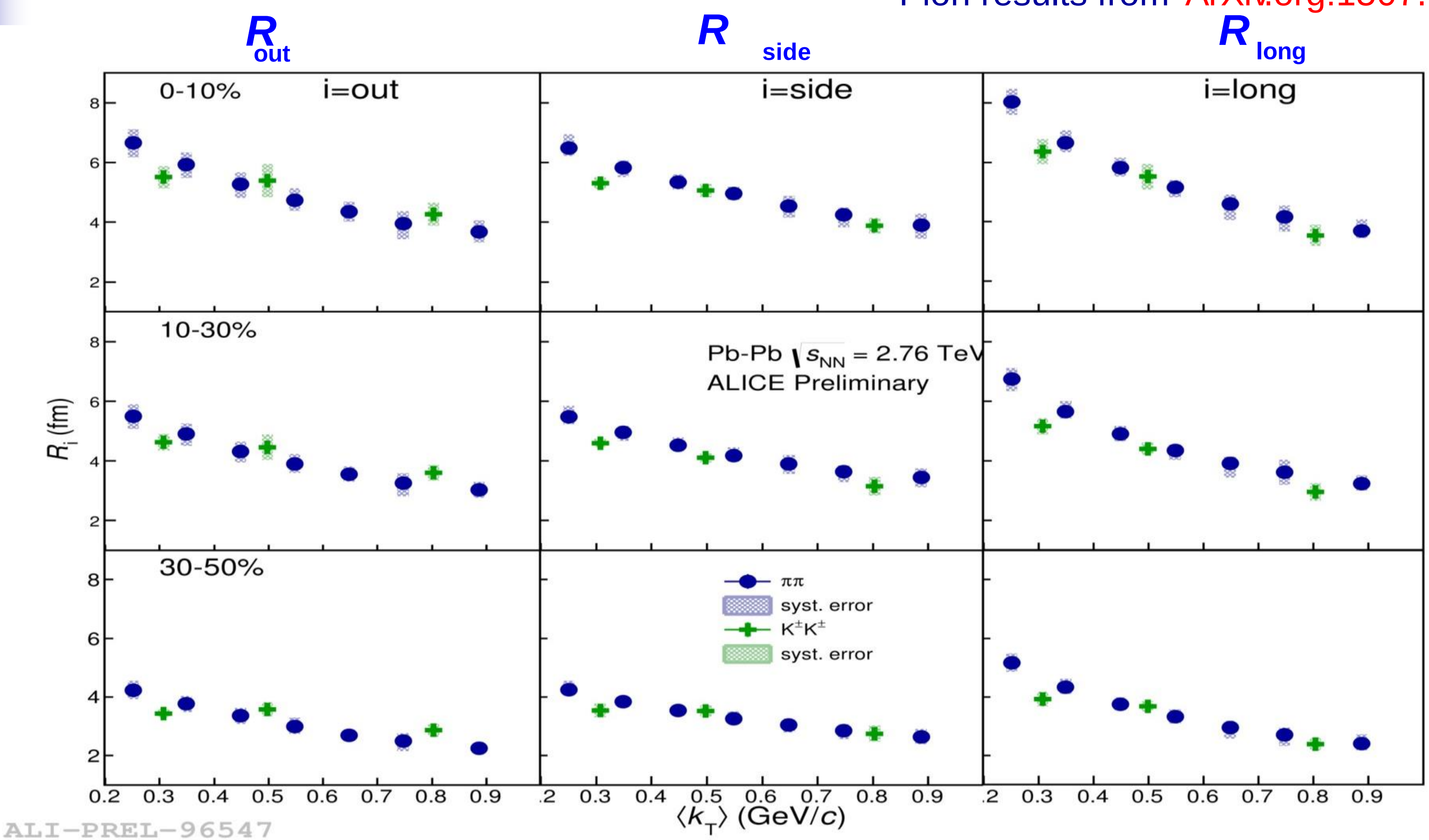

- Radii scale better with k_T than m_T according with HKM (V. Shapoval, P. Braun-Munzinger, Iu.A. Karpenko, Yu.M. Sinyukov, Nucl.Phys. A 929 (2014) 1);
- Similar observations were reported by PHENIX at RHIC (arxiv:1504.05168).

Space-time picture of the pion and kaon emission

$$\underbrace{R_l^2(k_T) = \tau^2\lambda^2\left(1+\frac{3}{2}\lambda^2\right)}_{2015} \approx \text{w/o transv. expansion} \approx \underbrace{\tau^2\frac{T}{m_T}}_{1987}\underbrace{\frac{K_2(\frac{m_T}{T})}{K_1(\frac{m_T}{T})}}_{1995}$$

where $\lambda^2 = \frac{T}{m_T}\left(1-\overbrace{\frac{k_T^2}{(m_T+\alpha T)^2}}^{\bar{v}_T^2}\right)^{1/2}$

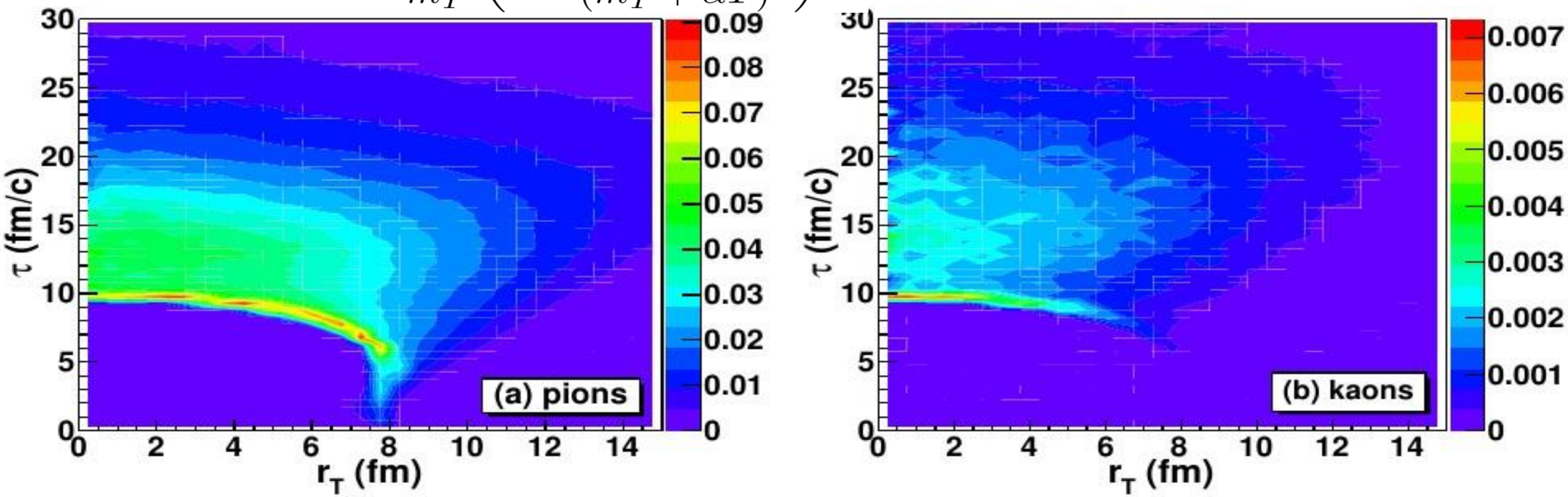

FIG. 4. The momentum angle averaged emission functions per units of space-time and momentum rapidities $g(\tau, r_T, p_T)$ [fm^{-3}] (see body text) for pions (a) and kaons (b) obtained from the HKM simulations of Pb+Pb collisions at the LHC $\sqrt{s_{NN}} = 2.76$ GeV, $0.2 < p_T < 0.3$ GeV$/c$, $|y| < 0.5$, $c = 0 - 5\%$. From Yu.S., Shapoval, Naboka, Nucl. Phys. A 946 (2016) 247 (arXiv:1508.01812)

Extraction of emission time from fit R_{long} T

- The new formula for extraction of the maximal emission time for the case of strong transverse flow was used (**Yu. S., Shapoval, Naboka, Nucl. Phys.** A 946 (2016) 227)

- The parameters of freeze-out: T and "intensity of transverse flow" α were fixed by fitting π and K spectra (arxiv:1508.01812)

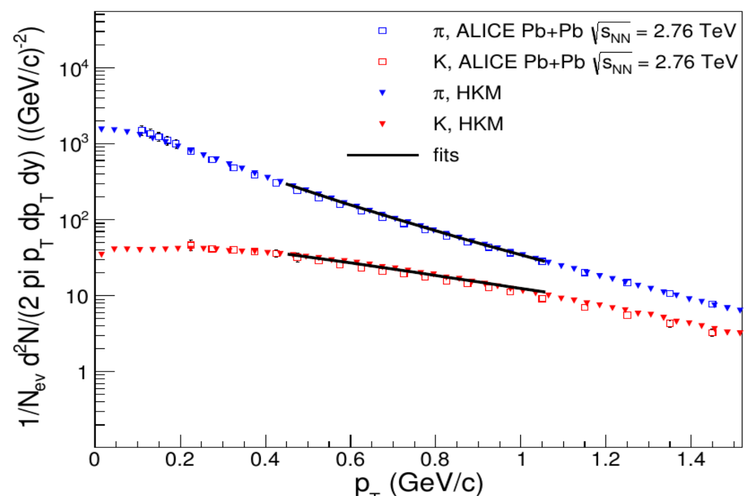

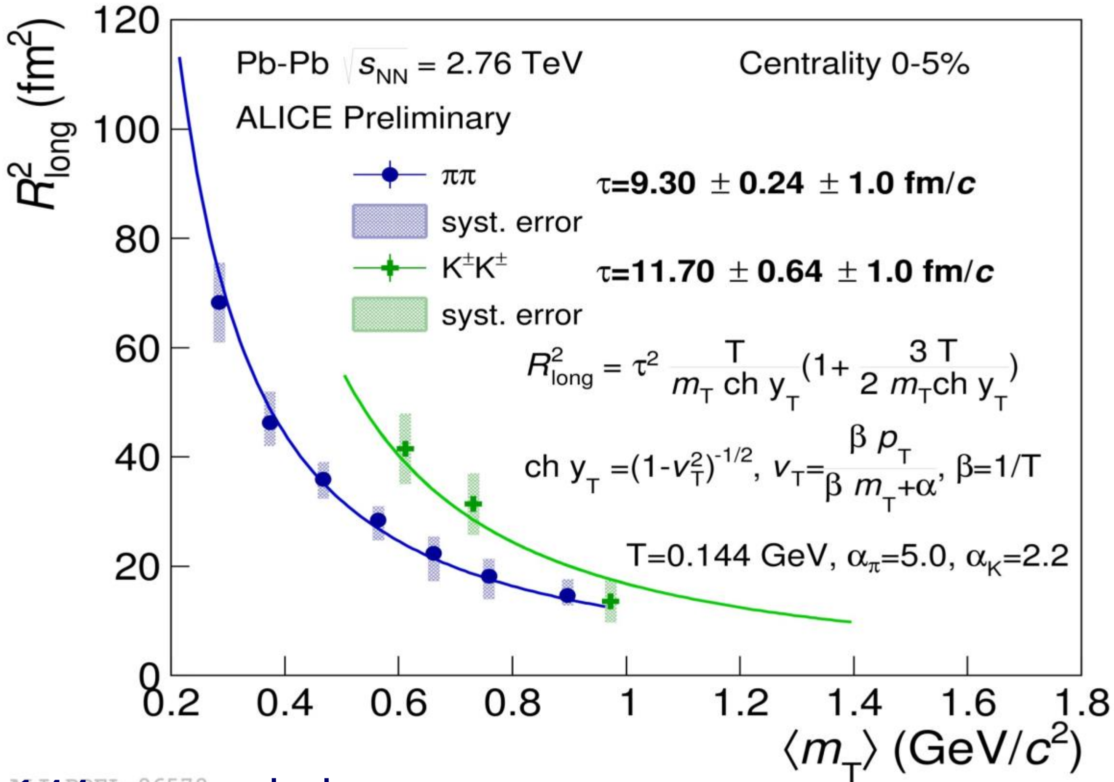

- To estimate the systematic errors: T = 0.144 was varied on ± 0.03 GeV &free α_π, α_K, were used; systematic errors ~ 1 fm/c

- Indication: $\tau_\pi < \tau_K$. Possible explanations (arxiv:1508.01812): HKM includes re-scatterings (UrQMD cascade): e.g. Kπ→K*(892)→Kπ, KN→K*(892)X; (K*(892) lifetime 4-5 fm/c) [πN→N*(Δ)X, N*(Δ)→πX (N*s(Δs)- short lifetime)]

K* probes

*K**(892) life time is 4.2 fm/c

$K^{*0} \to K^+\pi^-$ radiation picture in iHKM. Sudden vs continuous thermal freeze-out at the LHC.

V.Shapoval, P.Braun-Munzinger, Yu.S. Nuclear Physics A 968 (2017) 391

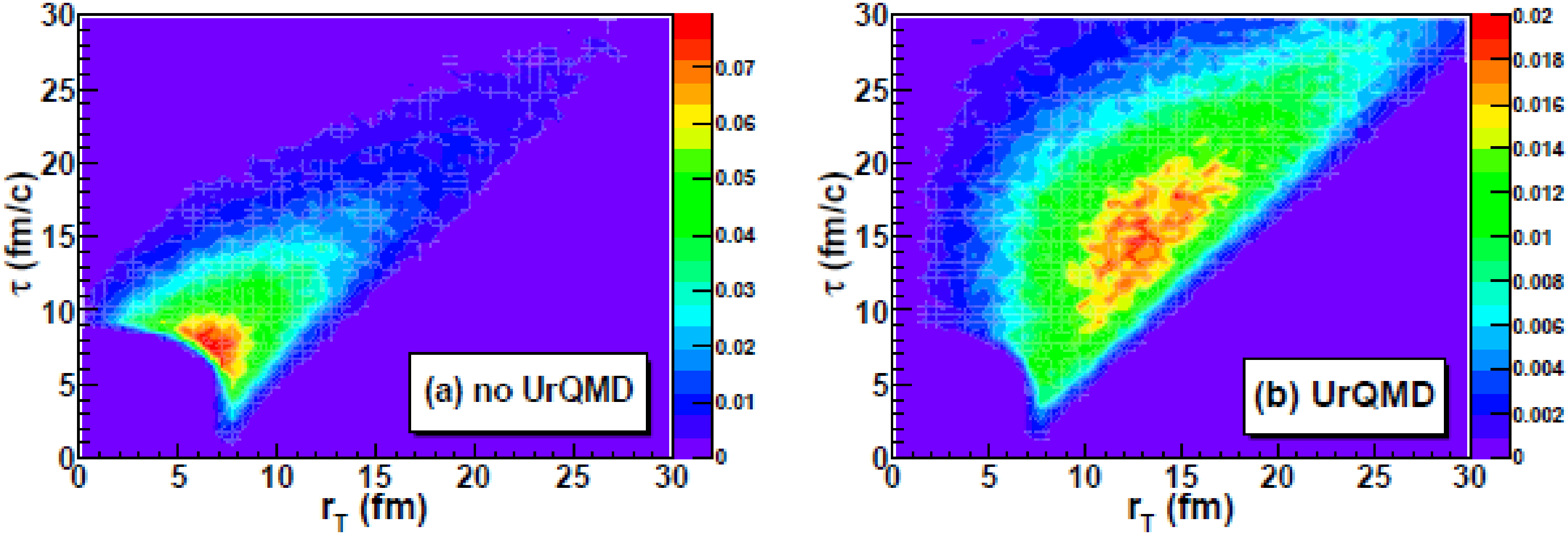

The comparison of the emission functions $g(\tau, r_T)$, averaged over complementary space and momentum components, of $K^+\pi^-$ pairs, associated with $K(892)^{*0}$ decay products, for two cases: (a) free-streaming of the particles and resonances, and (b) UrQMD hadron cascade. The plots are obtained using iHKM simulations of Pb+Pb collisions at the LHC $\sqrt{s_{NN}} = 2.76$ GeV, $0.3 < k_T < 5$ GeV$/c$, $|y| < 0.5$, $c = 5 - 10\%$.

$K^{*0} \to K^+\pi^-$ radiation picture in iHKM. Sudden vs continuous thermal freeze-out at the LHC.

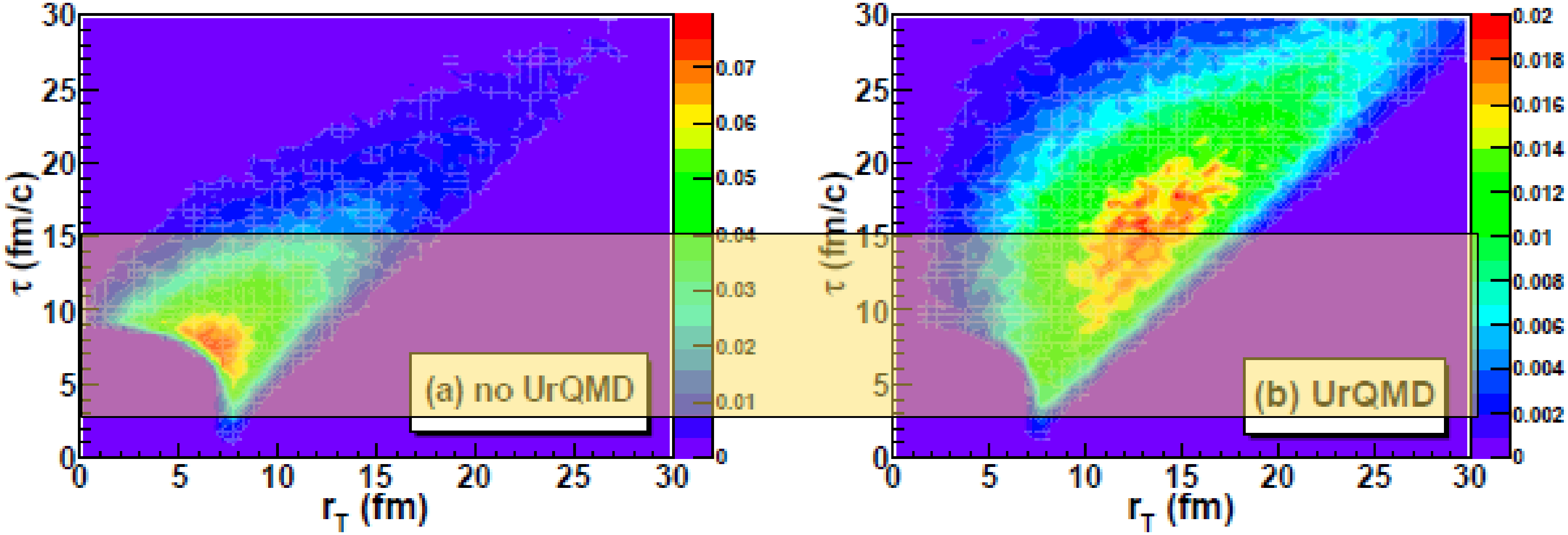

Less than 30% of direct K* can be seen till 15 fm/c

Suppression of K^{*0} due to continuous thermal freeze-out (LHC)

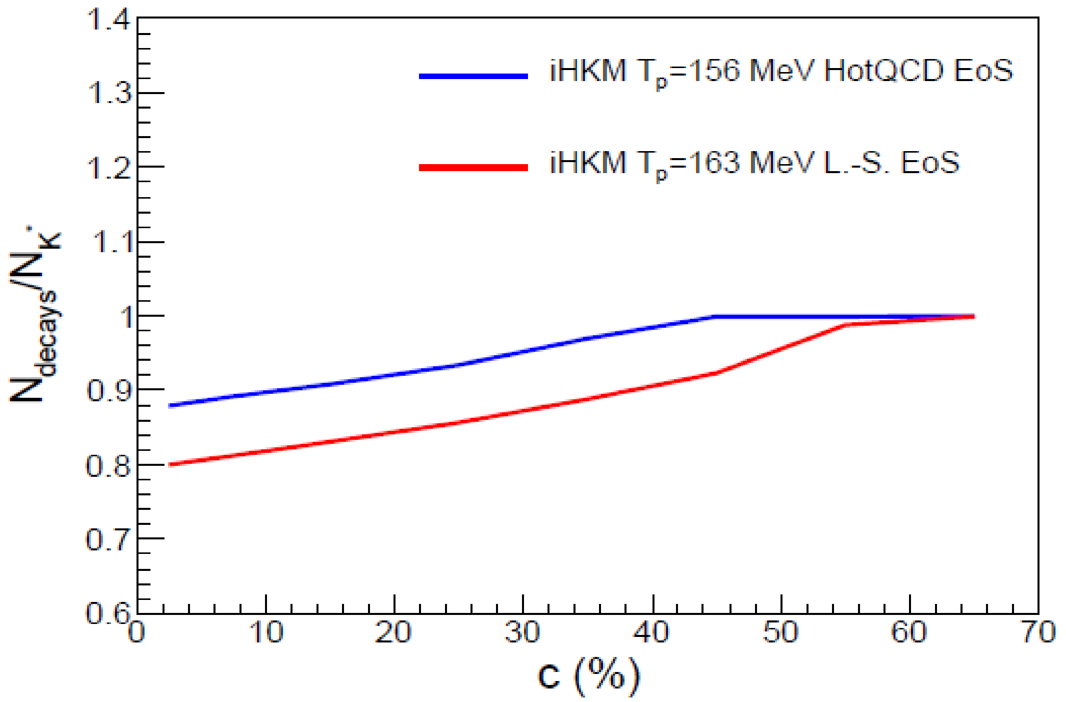

70% - 20% = 50%
Therefore
at least 50% of direct K^{*0} are recreated in reactions:

$$K^+\pi^- \to K^{*0}$$

FIG. 3. The fraction of $K^+\pi^-$ pairs coming from $K(892)^*$ decay, which can be identified as daughters of K^* in iHKM simulations after the particle rescattering stage modeled within UrQMD hadron cascade. The simulations correspond to LHC Pb+Pb collisions at $\sqrt{s_{NN}} = 2.76$ TeV with different centralities. The iHKM results are presented for two cases: the Laine-Shroeder equation of state with particlization temperature $T_p = 163$ MeV (red line) and the HotQCD equation of state with $T_p = 156$ MeV (blue line).

Spectra of K^{*0} (LHC)

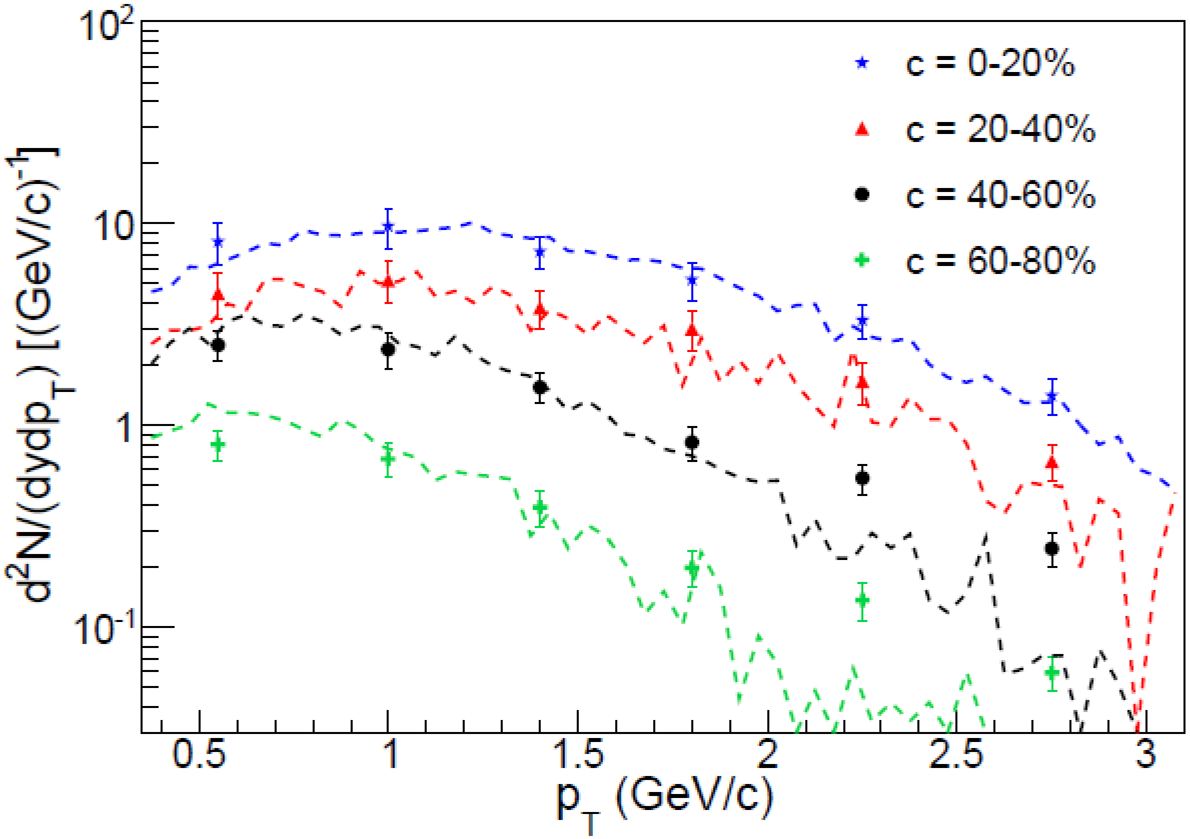

The $K(892)^*$ resonance p_T spectra for Pb+Pb collision events with different centralities at the LHC energy $\sqrt{s_{NN}} = 2.76$ TeV obtained in iHKM simulations (lines) in comparison with the experimental data [6] (markers).

Spectra of ϕ (LHC)

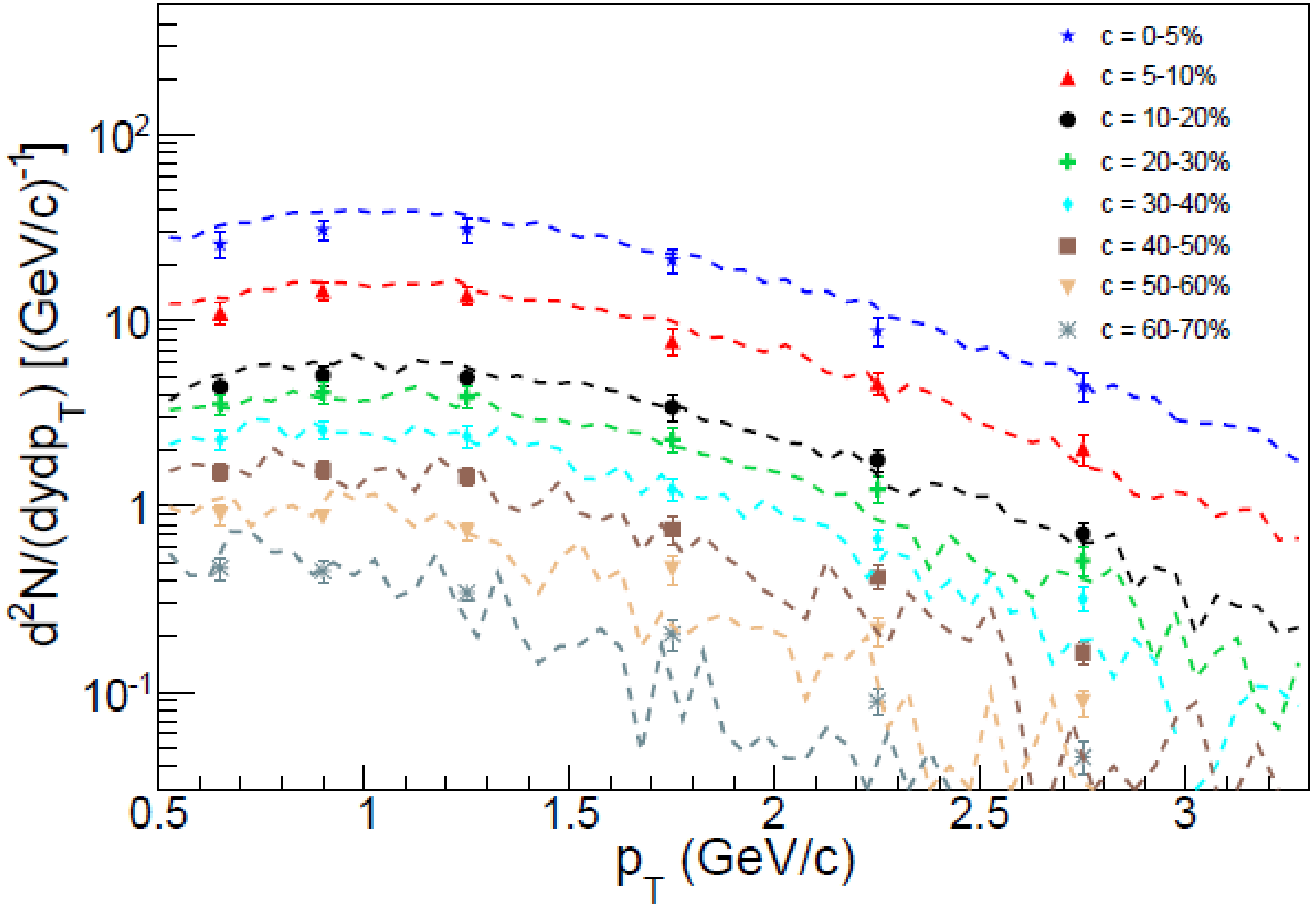

The $\phi(1020)$ resonance p_T spectra for Pb+Pb collision events with different centralities at the LHC energy $\sqrt{s_{NN}} = 2.76$ TeV obtained in iHKM simulations (lines) in comparison with the experimental data [6] (markers).

Thermal and evolutionary approaches

Continuous freeze-out **vs** sudden freeze-out

- Thermal models of particle production **vs** dynamic/evolutionary approaches

Kinetic/thermal freeze-out

Sudden freeze-out

Cooper-Frye prescription

$$p^0 \frac{d^3 N_i}{d^3 p} = \int_{\sigma_{th}} d\sigma_\mu p^\mu f_i(x,p)$$

The σ_{th} is typically isotherm.

Continuous freeze-out

$$p^0 \frac{d^3 N_i}{d^3 p} = \int d^4 x S_i(x,p) \approx \int_{\sigma(p)} d\sigma_\mu p^\mu f_i(x,p)$$

The $\sigma(p)$ is peace of hypersurface where the particles with momentum near p has a maximal emission rate. *Yu.S.* Phys. Rev. C78,

Chemical freeze-out

$$N_i = \int_p \int_{\sigma_{ch}} \frac{d^3 p}{p^0} d\sigma_\mu p^\mu f_i\left(\frac{p^\mu u_\mu(x)}{T_{ch}}, \frac{\mu_{i,ch}}{T_{ch}}\right)$$

$$= n_i(T,\mu) V_{eff} \qquad V_{eff} = \int_{\sigma_{ch}} u^\mu d\sigma_\mu$$

The numbers of quasi-stable particles is defined from N_i with taking into account the resonance decays but **not** inelastic re-scattering.

The T_{ch} is the minimal temperature when the expanding system is still (near) in local thermal and chemical equilibrium. Below the hadronic cascade takes place: $T_{ch} \rightarrow T_{part}$. The inelastic reactions, annihilation processes in hadron-resonance gas change the quasi-particle yields in comparison with sudden chem. freeze-out.

Equations of state

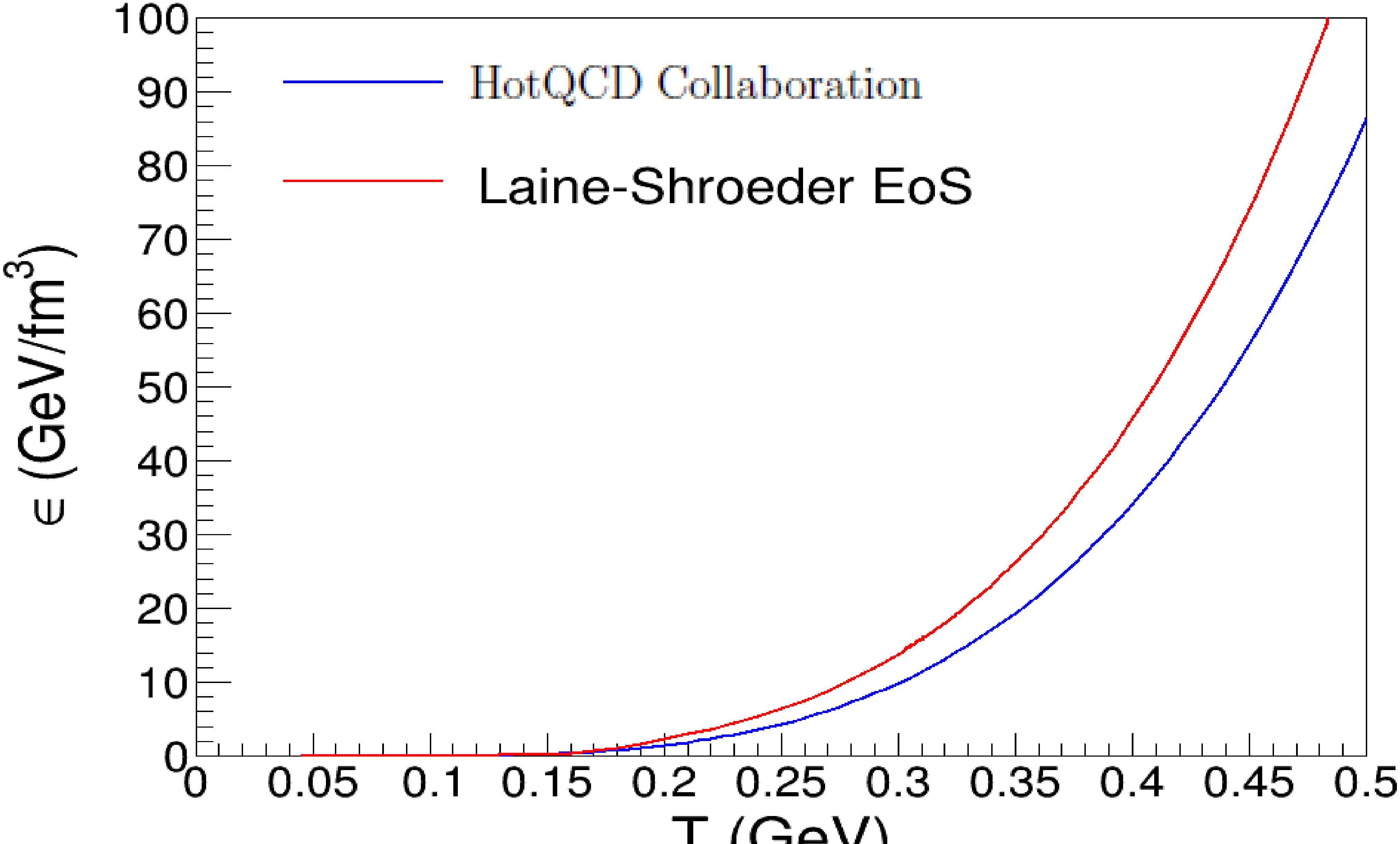

Multiplicity dependence of all charged particles on centrality and spectra for LHC energy $\sqrt{s_{NN}} = 2.76\ \text{TeV}$

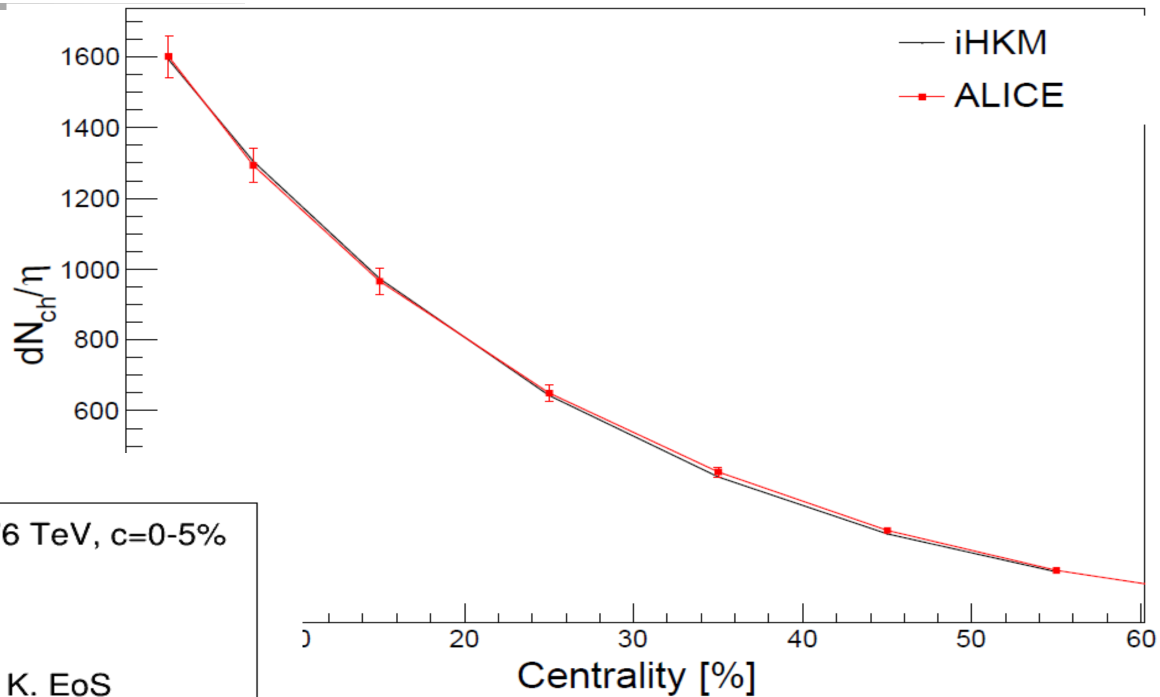

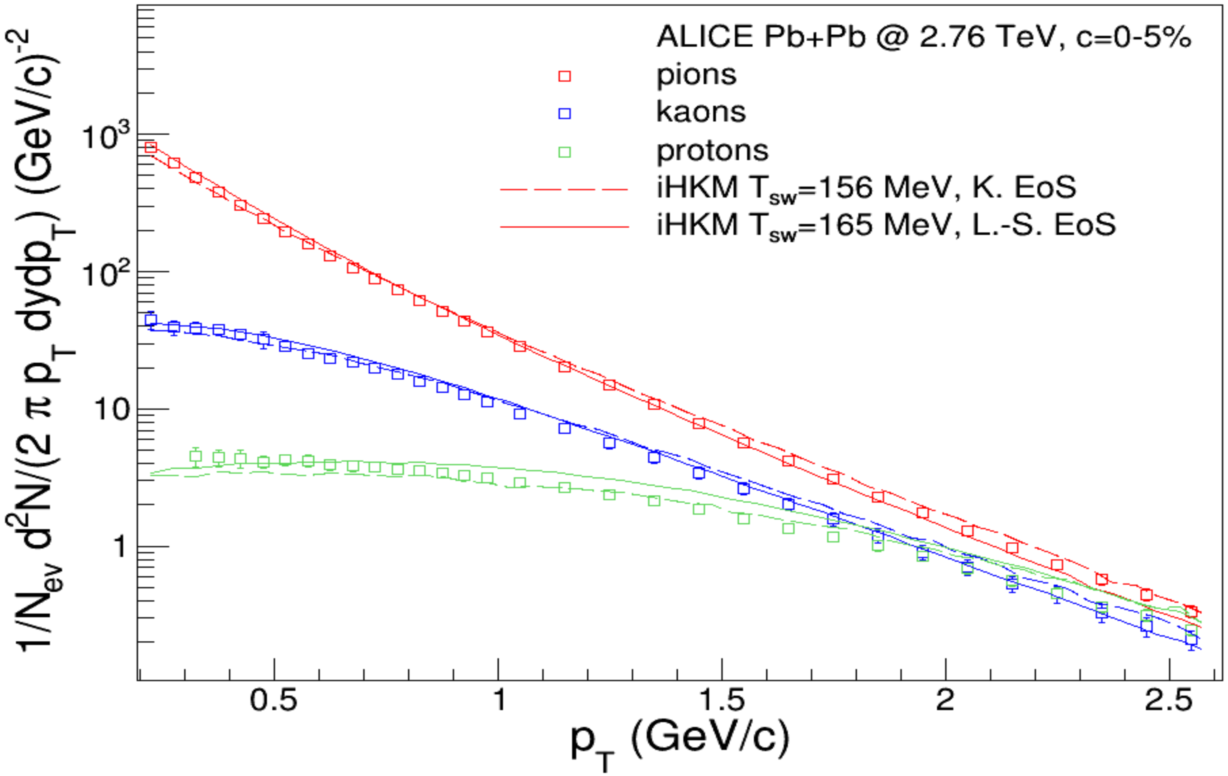

Thermal models **vs** evolutionary approach

Basic matter properties: thermodynamic **EoS**

Thermal models

Chemical freeze-out at $T_{ch} \approx T_h$

Particle number ratios $\{\frac{N_i}{N_j}\}$

Evolutionary models

$\frac{dN_{charge}}{d\eta}(c)$, $\frac{dN_\pi}{p_T dp_T}$ → High dense matter formation time τ_0; Max. energy density $\epsilon(\tau_0) \equiv \epsilon_0$

At the particlization temperature $T_{part} \approx T_h$ hydrodynamic evolution transforms (suddenly or continuously) into interact. hadron gas evolution.

EoS:

L.-S. → Karsch, Fodor (lattice QCD)

$T_h = 165 MeV \rightarrow 156 MeV$

$\tau_0 = 0.1$ fm/c → 0.15 fm/c

$\epsilon_0 = 679$ GeV/fm^3 → 495 GeV/fm^3

iHKM

Kinetic freeze-out

«Blast-wave" parametrization of sharp freeze-out hypersurface and transverse flows on it. Spectra $\frac{dN_i}{p_T dp_T} \rightarrow T_{th}$

"Effective temperature" of maximal emission: $T_{th}(p)$ Anyway the kinetic freeze-out in evolutionary models is continuous, how can we check it?

Particle number ratios at the LHC, Lattice EoS

Yu.S. , Shapoval, arXiv:1708.02389

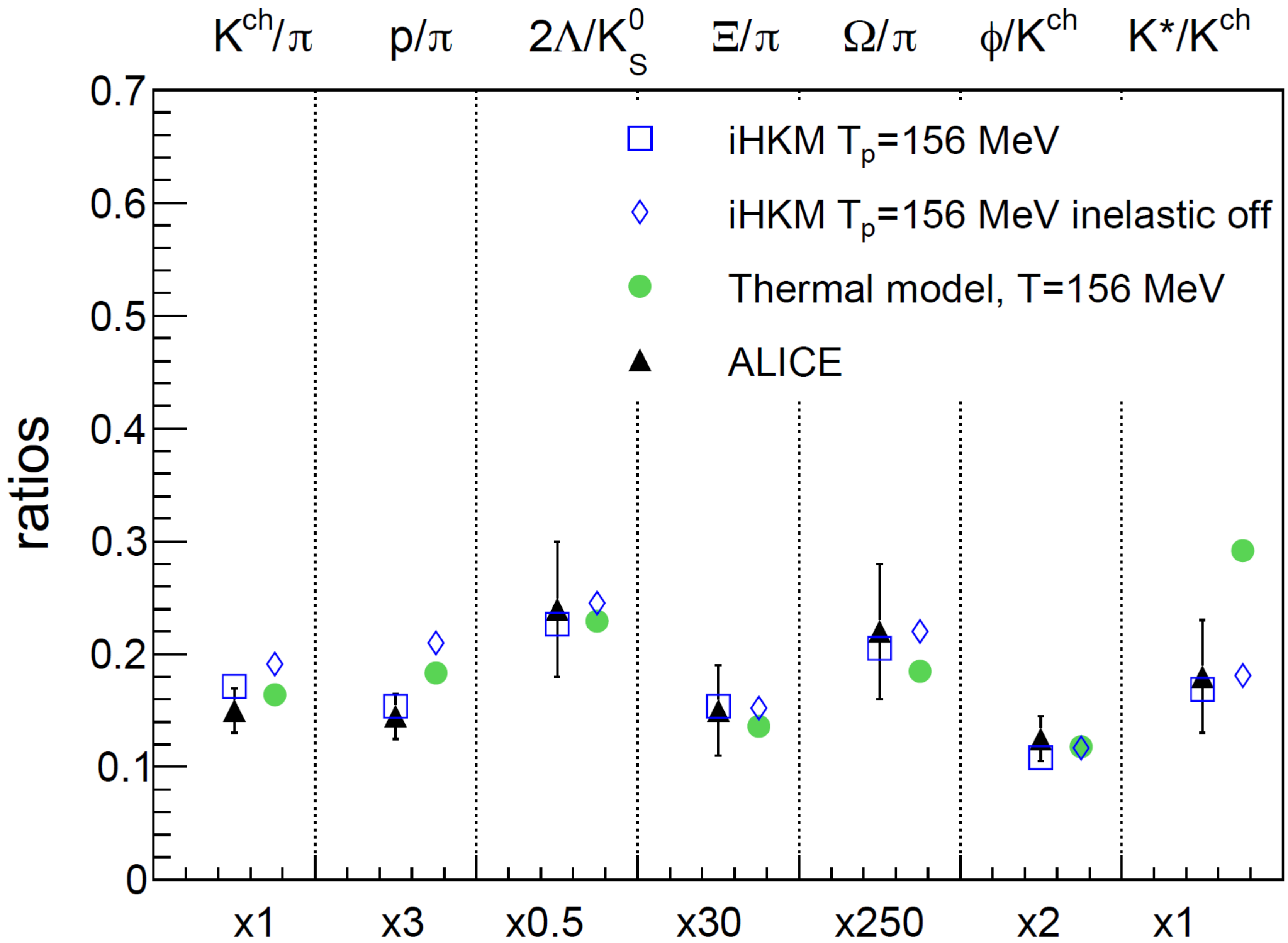

Particle number ratios at the LHC, L-S EoS

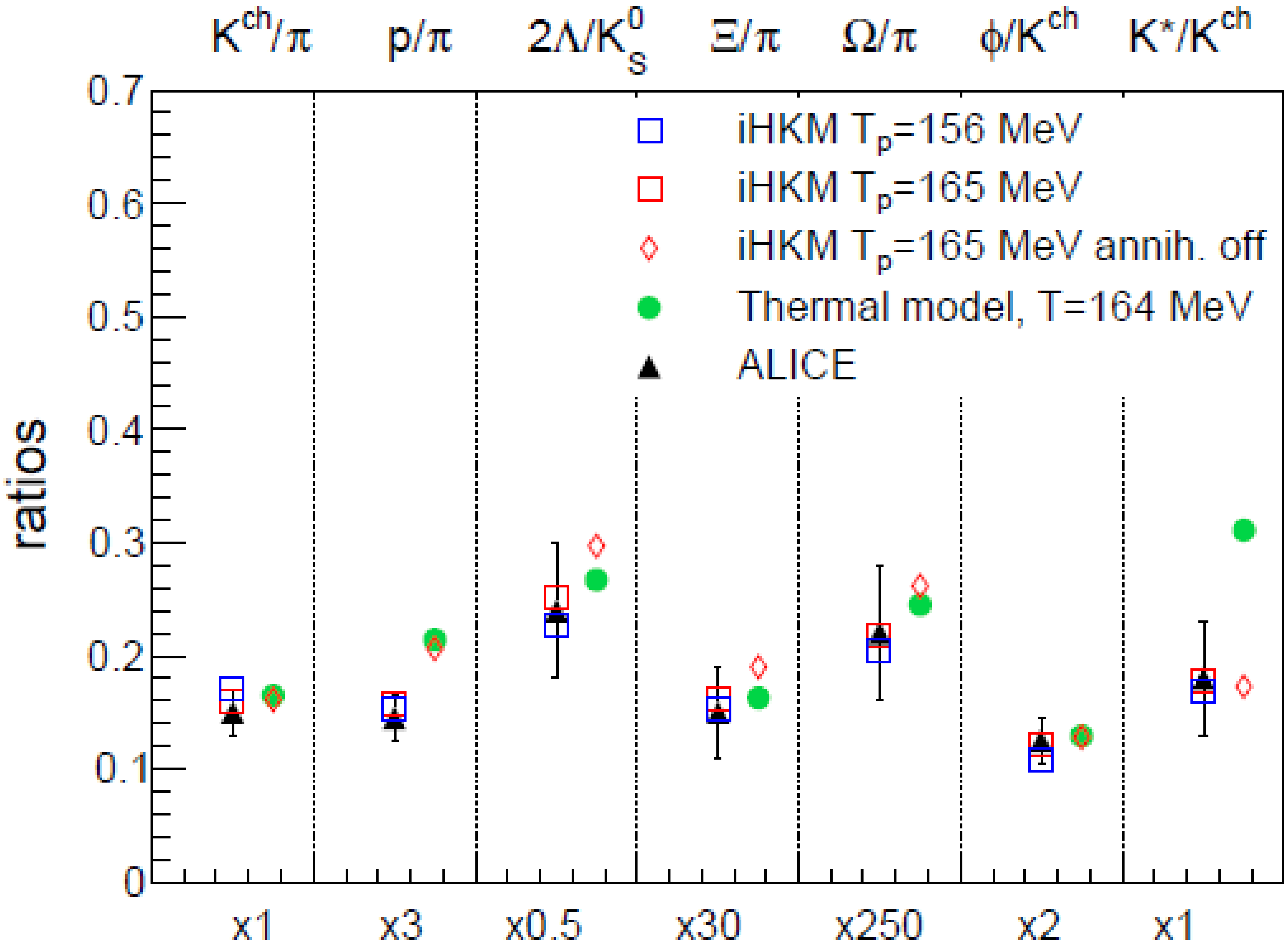

Yu.S. , Shapoval, arXiv:1708.02389

Summary on the particle production

- Neither thermal nor chemical freeze-out cannot be considered as sudden at some corresponding temperatures.

- Particle yield probe $\frac{dN_i}{d\eta}/\frac{dN_j}{d\eta}$ as well as absolute values $\frac{dN_i}{d\eta}$!) demonstrate that even at the minimal hadronization temperature $T_{ch} = T_h = 156$ MeV, the annihilation and other non-elastic scattering reactions play role in formation particle number ratios, especially.

- It happens that the results for small and relatively large T_h are quite similar. It seems that inelastic processes (other than the resonance decays), that happen at the matter evolution below T_h play a role of the compensatory mechanism in formation of $\frac{dN_i}{d\eta}/\frac{dN_j}{d\eta}$. Chemical freeze-out is continuous.

- As for the thermal freeze-out, the $K^{*0}(892)$ probes demonstrate that even at the first 4-5 fm/c (proper time!) after hadronization **at least** 70% of decay products are re-scattered. The intensive re-generation of K* takes place. **At least** 50% of direct $K^{*0}(892)$ are re-combine.

- About 30% of much longer-long-lived resonances $\phi(1020)$ with hidden strange quark content created additionally to direct $\phi(1020)$ (coming from hadronization) at the afterburner stage.

Acknowledgement

Щиро дякую усіх присутніх за їх присутність та увагу !

Thank you

СПАСИБО